

NASA TECHNICAL
MEMORANDUM

NASA TM X-53616

June 8, 1967

NASA TM X-53616

NATURAL ENVIRONMENT DESIGN CRITERIA GUIDELINES
FOR MSFC VOYAGER SPACECRAFT FOR
MARS 1973 MISSION

Edited by Don K. Weidner and C. L. Hasseltine
Aero-Astrodynamics Laboratory

NASA

*George C. Marshall
Space Flight Center,
Huntsville, Alabama*

N67-32399

FACILITY FORM 602	(ACCESSION NUMBER)	(PAGES)	(THRU)
	100		1
	(NASA CR OR TMX OR AD NUMBER)	(CODE)	31
		(CATEGORY)	

NATURAL ENVIRONMENT DESIGN CRITERIA GUIDELINES
FOR MSFC VOYAGER SPACECRAFT FOR MARS 1973 MISSION

Edited by

Don K. Weidner and C. L. Hasseltine

George C. Marshall Space Flight Center

Huntsville, Alabama

ABSTRACT

This document contains the natural environment information that is essential to the design of the Voyager spacecraft for the 1973 Mars mission. This information is based upon the results of inhouse studies and data taken from existing literature. As it would be impractical to make specific references to the literature utilized in the development of this report, only a bibliography of the reports used is given. The references contained in the documents listed in this bibliography were also used.

Since much of this information is in a state of flux because of the rapid advancement of the state-of-the-art, a continuing effort will be made to update and refine these specifications as later data become available. For more information relating to a specific environmental parameter, the reader should contact the Space Environment Branch of the Aerospace Environment Division.

NASA-GEORGE C. MARSHALL SPACE FLIGHT CENTER

N67 32399

NASA - GEORGE C. MARSHALL SPACE FLIGHT CENTER

Technical Memorandum X-53616

June 8, 1967

NATURAL ENVIRONMENT DESIGN CRITERIA GUIDELINES FOR MSFC
VOYAGER SPACECRAFT FOR MARS 1973 MISSION

Edited by

Don K. Weidner and C. L. Hasseltine

AERO-ASTRODYNAMICS LABORATORY
AEROSPACE ENVIRONMENT DIVISION
RESEARCH AND DEVELOPMENT OPERATIONS

TABLE OF CONTENTS

Section/ Paragraph	Title	Page
I	EARTH'S ENVIRONMENT	1 - 1
	1. 1 ATMOSPHERE	1 - 1
	1. 2 IONOSPHERE	1 - 3
	1. 3 MAGNETIC FIELD	1 - 6
	1. 4 RADIATION	1 - 13
	1. 4. 1 Thermal Radiation	1 - 13
	1. 4. 2 Magnetically Trapped Radiation	1 - 13
	1. 4. 3 Galactic Cosmic Radiation	1 - 13
	1. 4. 4 Solar Flares	1 - 23
	1. 5 GRAVITY	1 - 28
	1. 6 METEOROIDS	1 - 28
II	INTERPLANETARY ENVIRONMENT BETWEEN EARTH AND MARS	2 - 1
	2. 1 ATMOSPHERE	2 - 1
	2. 1. 1 Kinetic Gas Temperature	2 - 1
	2. 1. 2 Gas Pressure	2 - 1
	2. 1. 3 Density	2 - 1
	2. 2 SOLAR THERMAL RADIATION	2 - 3
	2. 3 MAGNETIC FIELD	2 - 4
	2. 4 GALACTIC COSMIC RADIATION	2 - 4
	2. 5 SOLAR COSMIC RADIATION	2 - 5
	2. 5. 1 Solar High Energy Particle Radiation	2 - 5
	2. 5. 2 Solar Flares	2 - 6
	2. 5. 3 Solar Wind	2 - 9
	2. 6 SOLAR RADIATION PRESSURE	2 - 10
	2. 7 METEOROIDS	2 - 11
III	MARTIAN ENVIRONMENT SURFACE TO 10 MARS RADII	3 - 1
	3. 1 CLIMATE	3 - 1

TABLE OF CONTENTS (cont'd)

Section/Paragraph	Title	Page
3.1.1	Surface Temperatures	3-1
3.1.2	Observed Seasonal Changes	3-5
3.2	ATMOSPHERE	3-8
3.2.1	Temperature	3-8
3.2.2	Composition and Molecular Weight	3-9
3.2.3	Surface Pressure	3-10
3.2.4	Model Atmospheres	3-10
3.2.5	Computed Quantities	3-11
3.2.6	Martian Winds	3-12
3.2.7	Clouds in the Martian Atmosphere	3-12
3.2.8	Blue Haze	3-36
3.3	IONOSPHERE	3-37
3.4	MAGNETIC FIELD	3-38
3.5	RADIATION	3-39
3.5.1	Solar Thermal Radiation	3-39
3.5.2	Magnetically Trapped Radiation	3-40
3.5.3	Galactic Cosmic Radiation	3-40
3.5.4	Solar Cosmic Radiation	3-41
3.6	METEOROIDS	3-42
3.7	GRAVITY	3-42
3.8	ALBEDO	3-44
	BIBLIOGRAPHY	4-1

LIST OF ILLUSTRATIONS

Figure No.	Title	Page
1 - 1	ELECTRON CONCENTRATIONS IN THE EQUATORIAL PLANE AS A FUNCTION OF ALTITUDE	1 - 5
1 - 2	IONOSPHERE THERMAL ENERGY SPECTRUM	1 - 7
1 - 3	ATMOSPHERIC ELECTRICAL CONDUCTIVITY ABOVE THE EARTH AS A FUNCTION OF ALTITUDE	1 - 8
1 - 4	SOLAR SPECTRUM ABOVE THE EARTH'S ATMOSPHERE AT 1 A. U.	1 - 14
1 - 5	THE R- λ FLUX MAP FOR AP5	1 - 16
1 - 6	THE R- λ FLUX MAP FOR AP4, SEPTEMBER 1963	1 - 17
1 - 7	THE R- λ FLUX MAP FOR AP2, SEPTEMBER 1963	1 - 18
1 - 8	THE R- λ FLUX MAP FOR AP1, BEFORE SEPTEMBER 23, 1963	1 - 19
1 - 9	THE R- λ FLUX MAP FOR AP3, SEPTEMBER 1963	1 - 20
1 - 10	THE R- λ FLUX MAP OF THE AE2 ENVIRONMENT	1 - 21
1 - 11	ELECTRON OMNIDIRECTIONAL FLUX MAP AE2 (ELECTRONS/cm ² /sec) AT THE GEOMAGNETIC EQUATOR	1 - 22
1 - 12	INTEGRAL-COSMIC-RAY ENERGY SPECTRUM AT EXTREMES OF THE SUNSPOT CYCLE	1 - 24

LIST OF ILLUSTRATIONS (cont'd)

Figure No.	Title	Page
1-13	PROBABILITY p, IN A MISSION LASTING d DAYS, OF THE OCCURRENCE OF ONE OR MORE SOLAR FLARES WITH FLUX GREATER THAN OR EQUAL TO N WITH ENERGIES GREATER THAN OR EQUAL TO 30 MeV	1 - 25
1-14	FLUX OF PARTICLES WITH ENERGIES EQUAL TO OR GREATER THAN 30 MeV FROM SOLAR FLARES DURING THE LAST SOLAR CYCLE	1 - 26
1-15	GEOMAGNETIC CUT-OFF MOMENTA FOR VERTICALLY INCIDENT PROTONS AND ALPHA PARTICLES AT THE EARTH'S SURFACE FOR VARIOUS GEOMAGNETIC LATITUDES	1 - 27
2-1	ELECTRON DENSITY AS A FUNCTION OF DISTANCE ABOVE THE SOLAR LIMB IN THE EQUATORIAL PLANE AT ABOUT THE TIME OF SUNSPOT MINIMUM	2 - 2
2-2	THE PROBABILITY, p, OF THE OCCURRENCE OF A FLARE WHOSE FLUX IS EQUAL TO OR GREATER THAN N, AND WHOSE INDIVIDUAL PARTICLE ENERGIES ARE EQUAL TO OR GREATER THAN 30 MeV	2 - 7
3-1	SEASONAL ISOTHERMS, SOUTHERN HEMISPHERE SUMMER	3 - 2
3-2	SEASONAL ISOTHERMS, SOUTHERN HEMISPHERE FALL	3 - 3
3-3	SEASONAL ISOTHERMS, SOUTHERN HEMISPHERE WINTER	3 - 3
3-4	VARIATIONS IN SUN-MARS AND SUN-EARTH DISTANCE	3 - 4

LIST OF ILLUSTRATIONS (cont'd)

Figure No.	Title	Page
3-5	DIURNAL VARIATION IN THE MARTIAN ATMOSPHERE AND GROUND TEMPERATURE	3-6
3-6	DIURNAL VARIATION IN THE MARTIAN TEMPERATURE PROFILE	3-6
3-7	IDEALIZED TEMPERATURE PROFILES	3-8
3-8	IDEALIZED MOLECULAR WEIGHT PROFILES	3-10
3-9	ACCELERATION OF GRAVITY ON EARTH AND MARS VERSUS ALTITUDE	3-13
3-10	GEOPOTENTIAL HEIGHT VERSUS GEOMETRIC ALTITUDE ON MARS	3-13
3-11	KINETIC TEMPERATURE	3-14
3-12	COMPARISON OF MEAN KINETIC AND MOLECULAR TEMPERATURE	3-14
3-13	ATMOSPHERIC DENSITY	3-15
3-14	ATMOSPHERIC PRESSURE	3-15
3-15	DENSITY SCALE HEIGHT	3-16
3-16	PRESSURE SCALE HEIGHT	3-16
3-17	COLUMNAR MASS	3-17
3-18	NUMBER DENSITY	3-17
3-19	ATMOSPHERIC MEAN FREE PATH	3-18
3-20	SPEED OF SOUND	3-18

LIST OF TABLES

Table No.	Title	Page
1 - 1	IONOSPHERIC ELECTRON DENSITY LAYERS	1 - 3
1 - 2	AVERAGE TOTAL MAGNETIC FIELD IN GAUSS	1 - 10
1 - 3	EARTH GEOMAGNETIC FIELD	1 - 12
1 - 4	SOLAR-SPECTRAL-IRRADIANCE DATA -0.22 TO 7.0 MICRONS	1 - 15
1 - 5	ORBITAL ELEMENTS FOR MAJOR METEOR STREAMS	1 - 31
2 - 1	VARIATION OF SOLAR CONSTANT WITH SOLAR DISTANCE	2 - 3
2 - 2	PROBABILITY OF PARTICLE ENCOUNTER VS MISSION LENGTH	2 - 10
3 - 1	LENGTH OF SEASONS FOR VARIOUS HELIO- CENTRIC LONGITUDES	3 - 1
3 - 2	A MEAN MODEL AND 99% CONFIDENCE ENVELOPE FOR THE MARS ATMOSPHERE	3 - 19
3 - 3	ESTIMATED NEAR SURFACE WINDS AND VERTICAL WIND SHEARS	3 - 34
3 - 4	MARTIAN CLOUDS	3 - 35
3 - 5	RADIATION VERSUS ALTITUDE	3 - 45
3 - 6	PLANETARY ALBEDO	3 - 45

SECTION I
EARTH'S ENVIRONMENT

1.1 ATMOSPHERE

The Earth atmosphere described by the Patrick Reference Atmosphere will be used as reference for all studies and analyses requiring atmospheric data below approximately 116 kilometers above the Earth's surface. Between approximately 116 kilometers and 1,000 kilometers above the Earth's surface, Jacchia's 1964 static diffusion model will be used to define required parameters. Between 1,000 kilometers and the magnetopause, the kinetic temperature will remain constant at the value attained at 1,000 kilometers; pressure will be assumed to be 10^{-10} dynes/cm² and the variation in pressure is considered negligible. The density, which decreases from the value at 1,000 kilometers, will be computed from the following equation:

$$\rho_z = \rho_{\infty} + (\rho_{1000} - \rho_{\infty}) \exp [b(z - 1000)], z > 1000$$

in which

ρ_z = density at an altitude of z kilometers

ρ_{∞} = limiting value of density at large altitudes = 10^{-23} gm/cm³,

the density of interplanetary space

b = a constant defined as $b = (\ln 10) \frac{d \log_{10} \rho}{dz}$ at 1000 km and

computed from tabular values of $\log_{10} \rho$

z = altitude in kilometers

The static diffusion model atmosphere requires the following solar activity dependent geophysical inputs:

- Either predicted or actual daily and 81-day mean values of the 10.7 centimeter (2800 MC/S) solar radio flux as recorded at Ottawa, Canada.
- Either a predicted or actual value of the three-hour equivalent planetary amplitude, a_p , for the period 8 hours prior to the time at which a density value is to be computed.

Location; day, month, and year; and altitude in kilometers are also required input data; however, if the program is used as a subroutine of an orbital decay program, these data can be provided by the main program.

Predicted or actual values of the geophysical data required for input will be provided by the Space Environment Branch, Aerospace Environment Division, Aero-Astroynamics Laboratory upon request.

Beyond approximately 500 kilometers above the Earth's surface, the magnitude of the effect of solar radiation pressure forces on the vehicle is comparable to the magnitude of density-induced drag effects; however, in general, the two effects do not act in the same direction. The solar radiation pressure ranges in value from 4.5×10^{-5} dynes/cm² for a black body to as high as 9×10^{-5} dynes/cm² for a perfectly reflecting body.

1.2 IONOSPHERE

The expression ionosphere refers to that part of the Earth's atmosphere that contains ions and free electrons in sufficient quantities to affect the propagation of radio waves. In general, during the day, electron density is a minimum in the polar regions, increases to a maximum about 15 degrees from the geomagnetic equator, and decreases to a secondary minimum at the geomagnetic equator. The ionosphere has a layered structure with distinct maxima of electron densities occurring in layers, the best known being called the D, E, F₁, and F₂ layers which are described as follows:

Table 1-1. IONOSPHERIC ELECTRON DENSITY

REGION	CONCENTRATION		ALTITUDE	
	Minimum	Maximum	Minimum	Maximum
D	$10/cm^3$	$10^4/cm^3$		90 km
E	$10^4/cm^3$	$2 \times 10^5/cm^3$	90 km	160 km
F ₁ (daytime)	$1 \times 10^5/cm^3$	$4 \times 10^5/cm^3$	160 km	200 km
F ₂	$2 \times 10^5/cm^3$	$3 \times 10^6/cm^3$	160 km	350 km

The D layer has a maximum at about solar noon and a variation with solar activity of about 2 orders of magnitude. The E layer has a large diurnal variation (2 orders of magnitude) and nearly disappears at night. Consequently, attenuation by the E layer on

communication signals is much less at night than during the day. E layer electron concentrations are roughly twice as large in summer as in winter. The F₁ layer has a large diurnal variation; it is absent at night and weakest in the winter and near the maximum of the sunspot cycle. The height of maximum electron concentrations changes with the latitude and the time of day for the F₂ layer. It also has a general trend that is high for high solar activity. The electron concentrations beyond the ionosphere are given in Figure 1-1.

Propagation of radio waves is a function of electron density. The value of the refractive index in turn is determined by the electron density. The value of the refractive index is determined by

$$\mu = \sqrt{1 - \frac{4\pi N_e e^2}{\epsilon_0 m_e \omega^2}}$$

and μ = refractive index

N_e = electron density

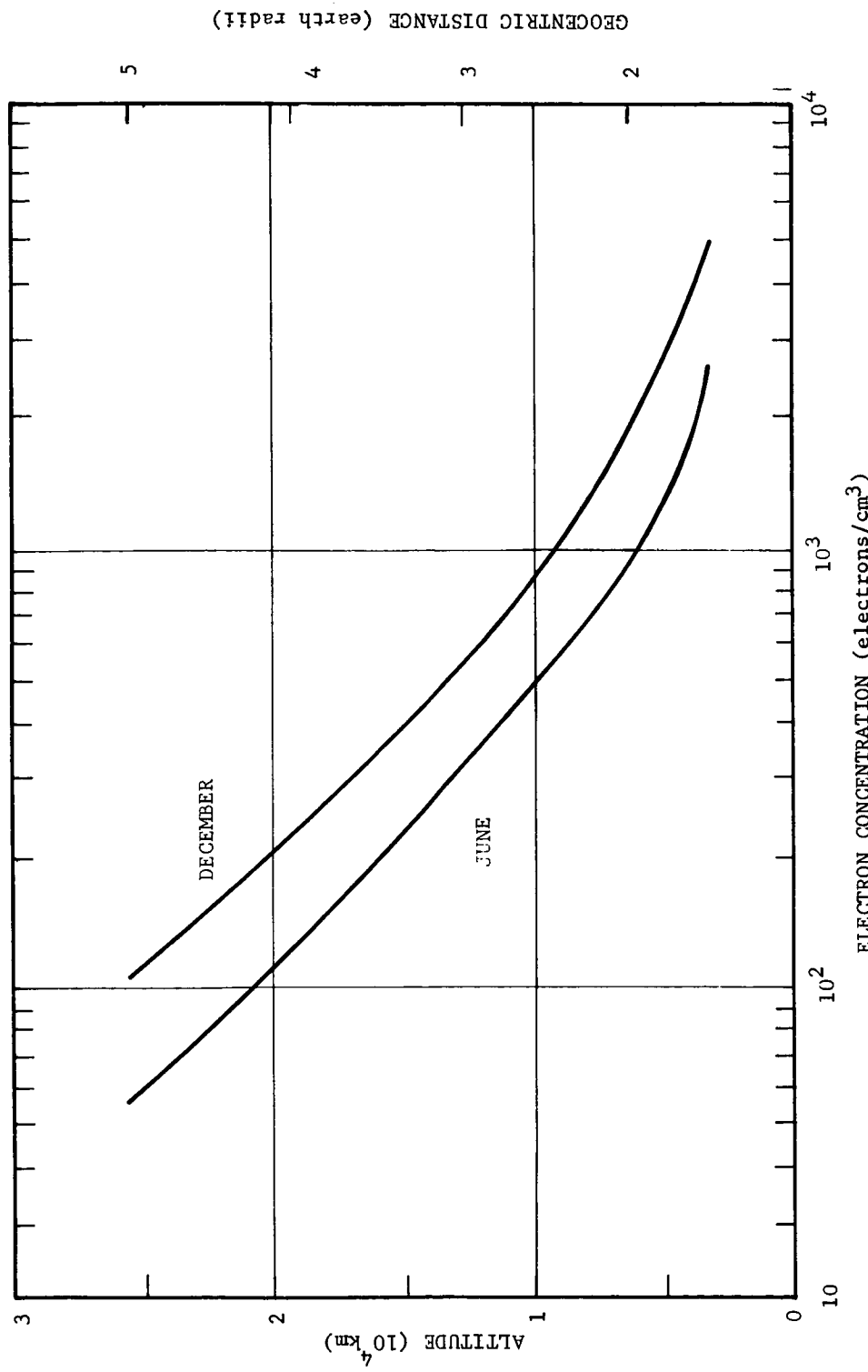
e_e = electron charge (coulombs)

m_e = electron mass (kg)

ω = angular frequency of the wave (radians/sec)

ϵ_0 = permittivity of free space (assuming the effects of ions are negligible).

Figure 1-1. ELECTRON CONCENTRATIONS IN THE EQUATORIAL PLANE AS A FUNCTION OF ALTITUDE



If μ^2 is negative, radio waves of frequencies corresponding to ω or lower will be reflected. The frequency that will just penetrate the F_2 layer (i.e., the layer having the highest electron density) is called the critical frequency, f_c . This gives

$$f_c = \sqrt{\frac{N_e e^2}{\pi \epsilon_0 m_e}} = 9 \times 10^{-3} \sqrt{N_e} \text{ mc/sec,}$$

where N_e is in electrons/cm³.

For satellite communications a frequency higher than f_c must be selected, and for the best signal strength possible, frequencies considerably higher than f_c (max) should be chosen. However, some investigations have indicated that the ionosphere may have resonance modes which could interfere significantly with even much higher frequency telemetry signals.

The ionospheric (thermal) energy spectrum is given in Figure 1-2. The average electrical conductivity in the ionosphere, based on measured data from satellites and probes, as a function of altitude, is given in Figure 1-3.

1.3 MAGNETIC FIELD

The Earth is surrounded by a magnetic field, often called the geomagnetic or terrestrial magnetic field, originating in its interior. The axis of the hypothetical magnet does not coincide with

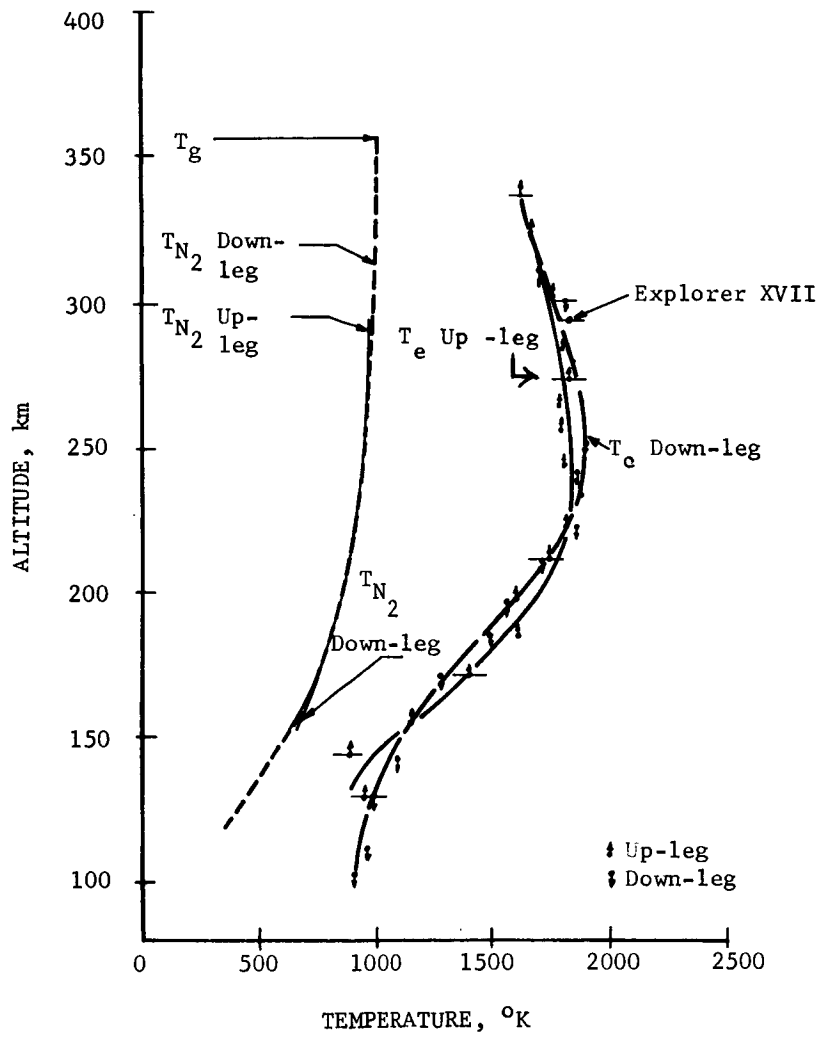


Figure 1-2. IONOSPHERE THERMAL ENERGY SPECTRUM. (Measured electron temperature (T_e), measured N₂ temperature (T_{N_2}), and neutral temperature (T_g). Computed from the Harris and Priester model. Wallops Island, April 18, 1963, 1604 e.s.t., $\chi = 60^\circ$, undisturbed conditions; 10.7 cm solar radiation flux = $100 \times 10^{-22} \text{ W/M}^2\text{-CPS.}$)

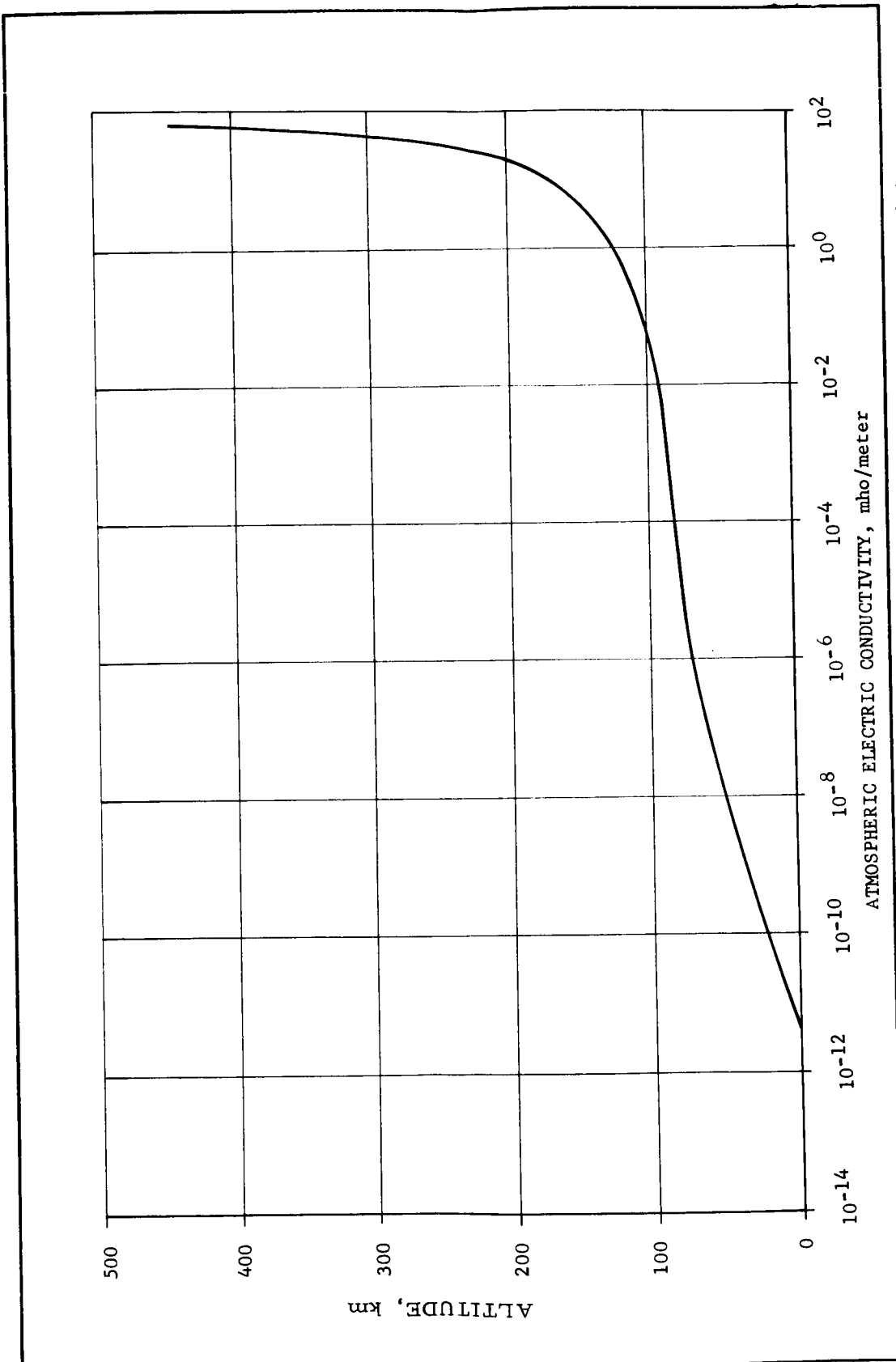


Figure 1-3. ATMOSPHERIC ELECTRICAL CONDUCTIVITY ABOVE THE EARTH AS A FUNCTION OF ALTITUDE (in absence of Earth's magnetic field.)

the north-south poles, and is displaced from the center by a distance of about 400 kilometers. Consequently, the geomagnetic field is not exactly symmetrical to the Earth's surface. The magnetic poles on the surface are the locations that, for all practical purposes, have the lines of force perpendicular to the surface.

The geomagnetic axis is a line joining the two magnetic poles. At the magnetic equator the lines of force are parallel everywhere to the Earth's surface; i.e., horizontal. From about 170° W, eastward to about 30° E, the geomagnetic equator is south, but at other longitudes it is north of the geographic equator.

The total strength of the Earth's magnetic field varies over the surface of the Earth, being 0.65 to 0.70 gauss near the magnetic poles and weakest toward the equatorial region where its value is 0.30 to 0.35 gauss. Its variation with latitude is by no means uniform, an exceptionally low value of 0.25 gauss having been recorded in southeast Brazil.

At some distance from the Earth, the intensity variation may be taken to be inversely proportional to the cube of the distance from the center of the dipole. The average total magnetic field is given in Table 1-2.

Table 1-2. AVERAGE TOTAL MAGNETIC FIELD IN GAUSS

Altitude (km)	Geodetic Colatitude in Degrees			
	0	30	60	80
200	.52243	.50782	.40338	.31406
400	.48121	.46403	.36670	.28630
1000	.37978	.35841	.28088	.21778
2000	.26428	.24682	.18904	.14629
3000	.19052	.17608	.13343	.10330
4000	.14158	.12988	.09773	.07571
6371.2	.07693	.07001	.05217	.04044

From measurements of the strength of the geomagnetic field, it is clear that the field is not a steady one but rather one with secular and transient variations. Secular variations require many years for the net effect to become significant. The transient variations, however, occur within days or less and are due to external factors, some of which are of solar origin.

The sun's emission of a solar plasma (i.e., the solar wind) influences the Earth's magnetic field. When the solar plasma enters the Earth's magnetic field, the interaction produces a sheath of current in the plasma which opposes, by Lenz's Law, the Earth's field.

The Earth's field is compressed until its magnetic pressure (i. e., its magnetic energy density) just balances the kinetic pressure of the solar plasma. This balance is reached at about 10 Earth radii, and therefore the Earth's magnetic field is to be limited to such a finite distance in a direction toward the sun. In directions that make an appreciable angle with the sun, the influence of the Earth's magnetic field will be extended considerably farther. Models for the magnetic field of the Earth, applicable to less than 10 Earth radii, are as given below:

The main geomagnetic field, out to six or seven Earth radii, can be derived from the magnetic potential formula

$$V = a \sum_{n=1}^{\infty} \sum_{m=0}^n \left(\frac{a}{r} \right)^m P_n^m (\cos \theta) (g_n^m \cos m\lambda + h_n^m \sin m\lambda)$$

by the straightforward evaluation of

$$\mathbf{F} = -\nabla V,$$

where a = mean radius of Earth; r = radial distance from Earth's center; θ = colatitude; λ = longitude East; V = magnetic potential; and $P_n^m (\cos \theta)$ = legendre functions.

Values of the coefficients g_n^m and h_n^m are given in Table 1-3.

Table 1-3. EARTH GEOMAGNETIC FIELD

Epoch 1960, GSFC(12/66) Set 1 Rounded

n	m	g_n^m	h_n^m	n	m	g_n^m	h_n^m
2	1	-30401.2	-0.	8	6	-3.6	24.3
2	2	-2163.8	5778.2	8	7	15.5	-22.5
3	1	-1540.1	-0.	8	8	3.6	-21.4
3	2	2997.9	-1932.0	9	1	8.5	0.
3	3	1590.3	202.9	9	2	6.5	5.4
4	1	1307.1	-0.	9	3	-9.3	-11.7
4	2	-1988.9	-425.4	9	4	-9.6	4.2
4	3	1276.8	227.8	9	5	-6.1	-15.3
4	4	881.2	-133.8	9	6	5.5	4.6
5	1	949.3	-0.	9	7	-8.1	21.9
5	2	803.5	160.3	9	8	13.0	-0.7
5	3	502.9	-274.3	9	9	7.4	-17.1
5	4	-397.7	2.3	10	1	10.4	0.
5	5	266.5	-246.6	10	2	5.8	-22.4
6	1	-233.5	-0.	10	3	7.5	13.8
6	2	355.7	5.1	10	4	-15.1	6.3
6	3	228.4	117.8	10	5	12.1	-3.0
6	4	-28.8	-114.8	10	6	4.7	-1.9
6	5	-157.9	-108.9	10	7	0.2	9.0
6	6	-62.2	82.4	10	8	1.6	11.5
7	1	49.2	-0.	10	9	0.9	0.1
7	2	57.5	-12.1	10	10	0.2	-1.5
7	3	-0.8	104.4	11	1	-2.9	0.
7	4	-238.3	56.6	11	2	-0.9	-0.1
7	5	-1.5	-23.4	11	3	-2.2	4.5
7	6	-2.0	-14.8	11	4	0.8	-1.0
7	7	-108.9	-13.3	11	5	-2.8	2.6
8	1	72.2	-0.	11	6	6.4	-4.4
8	2	-53.7	-53.7	11	7	4.7	-1.3
8	3	7.9	-27.4	11	8	-0.2	-3.6
8	4	15.6	-8.1	11	9	1.8	4.0
8	5	-24.3	7.0	11	10	2.0	1.0
				11	11	1.1	-2.0

1.4 RADIATION

1.4.1 Thermal Radiation

The solar spectrum at 1 AU is given in Figure 1-4. The "Johnson Curve" is tabulated for easy reference in Table 1-4. The value of the solar constant at 1 AU is 1400 watts/m^2 .

1.4.2 Magnetically Trapped Radiation

The detailed data provided in NASA SP-3024 will be used, with the caution that these data are time-averaged and, particularly in the case of outer zone electrons, do not represent the maximum hazard model.

1.4.2.1 Protons. Geomagnetically trapped proton environment may be shown by Figures 1-5, -6, -7, -8, and -9, where R = geocentric radius of particle flux and λ = geomagnetic latitude.

1.4.2.2 Electrons. Geomagnetically trapped electron fluxes with energies greater than 500 KeV are depicted in Figure 1-10. The energy spectrum is shown in Figure 1-11.

1.4.3 Galactic Cosmic Radiation

- Composition:
 - ~ 85% protons (H^+)
 - ~ 14% alpha particles (He^{++})
 - ~ 1% nuclei of elements Li → Fe
(in approximately cosmic abundance)
- Flux at sunspot maximum: ~ 4 protons/cm² - sec
(isotropic)

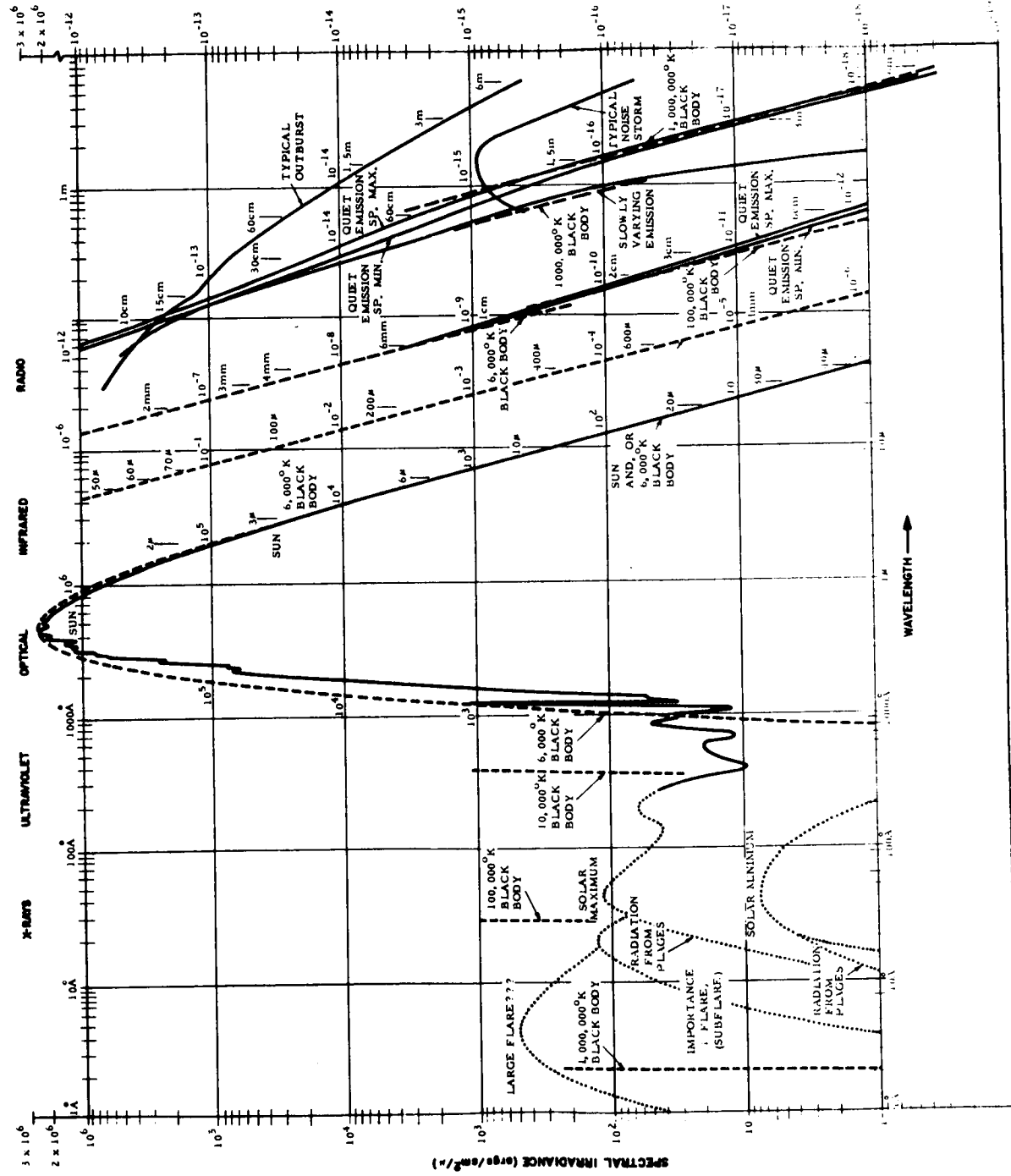
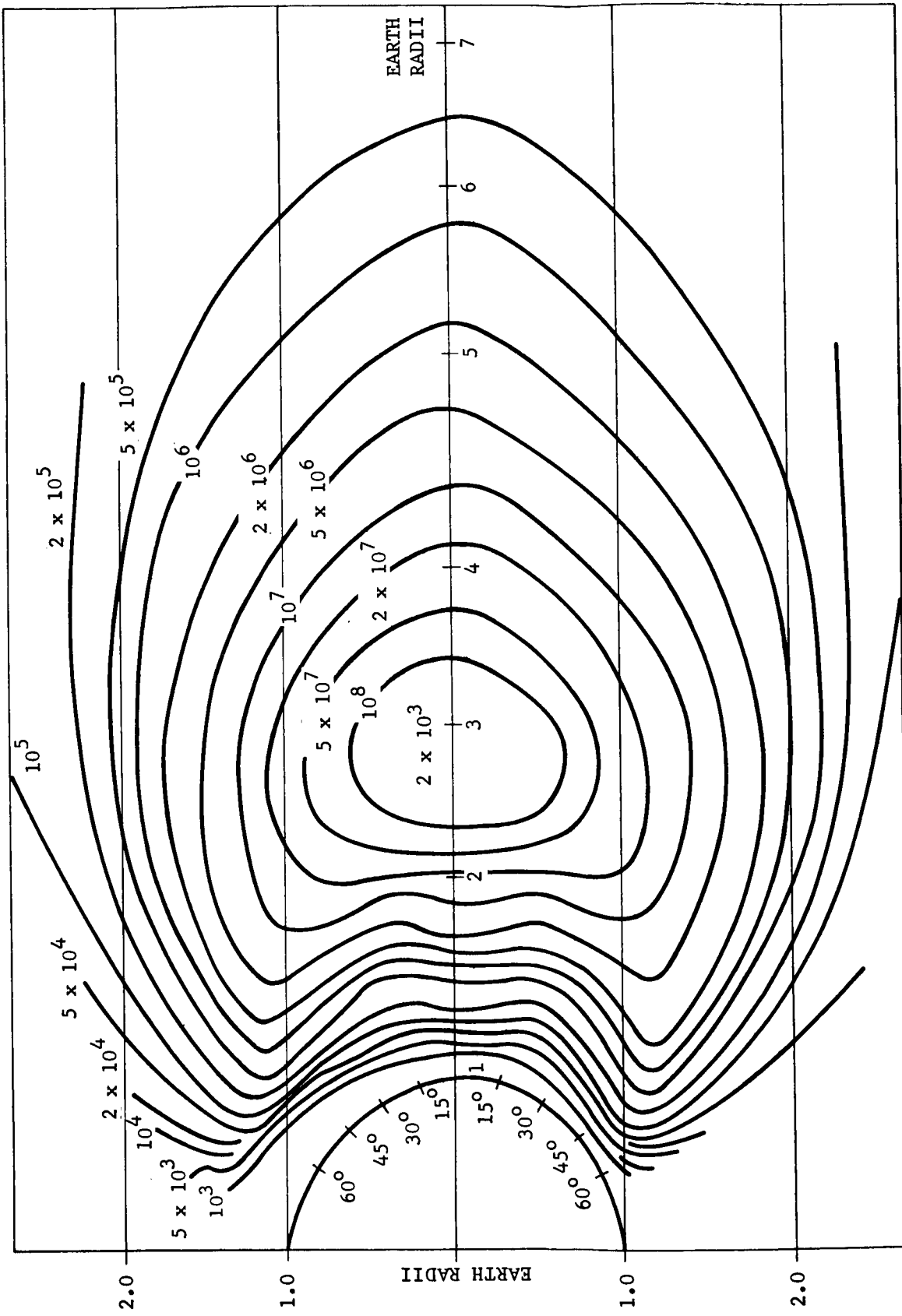


Figure 1-4. SOLAR SPECTRUM ABOVE THE EARTH'S ATMOSPHERE AT 1 A. U.

Table 1-4. SOLAR-SPECTRAL-IRRADIANCE DATA - 0.22 TO 7.0 MICRONS

λ (μ)	H_λ (w/cm ² μ)	P_λ (%)	λ (μ)	H_λ (w/cm ² μ)	P_λ (%)	λ (μ)	H_λ (w/cm ² μ)	P_λ (%)	λ (μ)	H_λ (w/cm ² μ)	P_λ (%)
0.22	0.0062	0.06	0.395	0.120	8.60	0.57	0.187	33.2	1.9	0.01274	93.02
0.225	0.0070	0.08	0.40	0.154	9.08	0.575	0.187	33.9	2.0	0.01079	93.87
0.23	0.0072	0.11	0.405	0.188	9.70	0.58	0.187	34.5	2.1	0.00917	94.58
0.235	0.0064	0.14	0.41	0.194	10.3	0.585	0.185	35.2	2.2	0.00785	95.20
0.24	0.0068	0.16	0.416	0.192	11.0	0.59	0.184	35.9	2.3	0.00676	95.71
0.245	0.0078	0.18	0.42	0.192	11.7	0.595	0.183	36.5	2.4	0.00585	96.18
0.25	0.0076	0.21	0.425	0.189	12.4	0.60	0.181	37.2	2.5	0.00509	96.57
0.255	0.0112	0.25	0.43	0.178	13.0	0.61	0.177	38.4	2.6	0.00445	96.90
0.26	0.014	0.29	0.435	0.182	13.7	0.62	0.174	39.7	2.7	0.00390	97.21
0.265	0.020	0.35	0.44	0.203	14.4	0.63	0.170	40.9	2.8	0.00343	97.47
0.27	0.025	0.42	0.445	0.215	15.1	0.64	0.166	42.1	2.9	0.00303	97.72
0.275	0.022	0.51	0.45	0.220	15.9	0.65	0.162	43.3	3.0	0.00268	97.90
0.28	0.024	0.59	0.455	0.219	16.7	0.66	0.159	44.5	3.1	0.00230	98.08
0.285	0.034	0.70	0.46	0.216	17.5	0.67	0.155	45.6	3.2	0.00214	98.24
0.29	0.052	0.85	0.465	0.215	18.2	0.68	0.151	46.7	3.3	0.00191	98.39
0.295	0.063	1.06	0.47	0.217	19.0	0.69	0.148	47.8	3.4	0.00171	98.52
0.30	0.061	1.30	0.475	0.220	19.8	0.70	0.144	48.8	3.5	0.00153	98.63
0.305	0.067	1.50	0.48	0.216	20.6	0.71	0.141	49.8	3.6	0.00139	98.74
0.31	0.076	1.66	0.485	0.203	21.3	0.72	0.137	50.8	3.7	0.00125	98.83
0.315	0.082	2.03	0.49	0.199	22.0	0.73	0.134	51.8	3.8	0.00114	98.91
0.32	0.085	2.32	0.495	0.204	22.8	0.74	0.130	52.7	3.9	0.00103	98.99
0.325	0.102	2.66	0.50	0.198	23.5	0.75	0.127	53.7	4.0	0.00095	99.05
0.33	0.115	3.08	0.505	0.197	24.2	0.80	0.1127	57.9	4.1	0.00087	99.13
0.335	0.111	3.46	0.51	0.196	24.9	0.85	0.1003	61.7	4.2	0.00080	99.18
0.34	0.111	3.86	0.515	0.189	25.6	0.90	0.895	65.1	4.3	0.00073	99.23
0.345	0.117	4.27	0.52	0.187	26.3	0.95	0.0803	68.1	4.4	0.00067	99.29
0.35	0.118	4.69	0.525	0.192	26.9	1.0	0.0725	70.9	4.5	0.00061	99.33
0.355	0.116	5.10	0.53	0.195	27.6	1.1	0.0606	75.7	4.6	0.00056	99.38
0.36	0.116	5.53	0.535	0.197	28.3	1.2	0.0501	79.6	4.7	0.00051	99.41
0.365	0.129	5.95	0.54	0.198	29.0	1.3	0.0406	82.9	4.8	0.00048	99.45
0.37	0.133	6.42	0.545	0.198	29.8	1.4	0.0328	85.5	4.9	0.00044	99.48
0.375	0.132	6.90	0.55	0.195	30.5	1.5	0.0267	87.6	5.0	0.00042	99.51
0.38	0.123	7.35	0.555	0.192	31.2	1.6	0.0220	89.4	6.0	0.00021	99.74
0.385	0.115	7.78	0.56	0.190	31.8	1.7	0.0182	90.83	7.0	0.00012	99.86
0.39	0.112	8.19	0.565	0.189	32.5	1.8	0.0152	92.03			

 λ = WAVELENGTH IN MICRONS, μ (10^{-6} M) H_λ = THERMAL RADIATION IN WATTS/CM² μ P_λ = PERCENT OF THERMAL SOLAR CONSTANT
WITH WAVELENGTHS LESS THAN λ



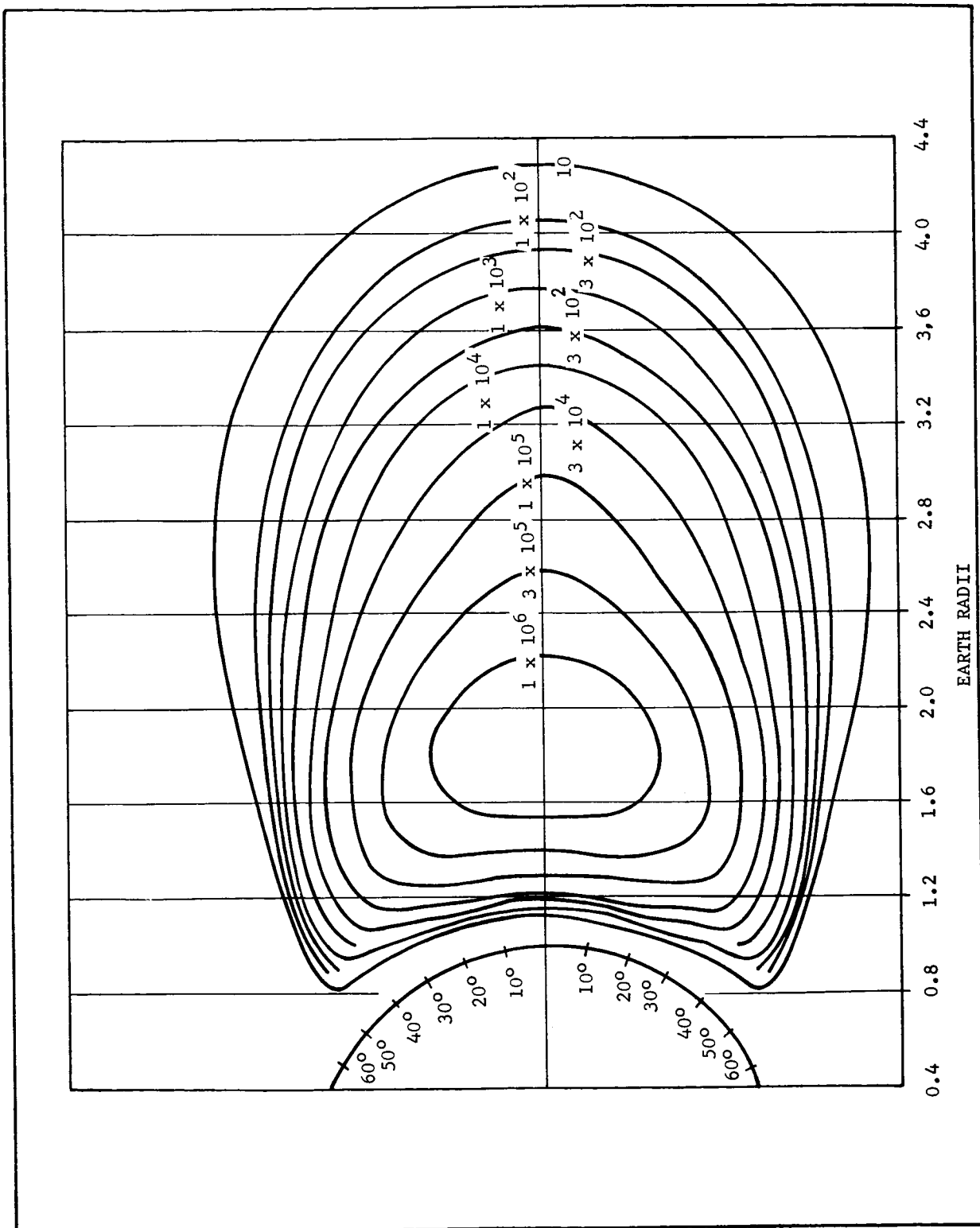


Figure 1-6. THE R- λ FLUX MAP FOR AP4, SEPTEMBER 1963 (The contours are the omnidirectional flux (protons/cm²-sec) above 4 MeV.)

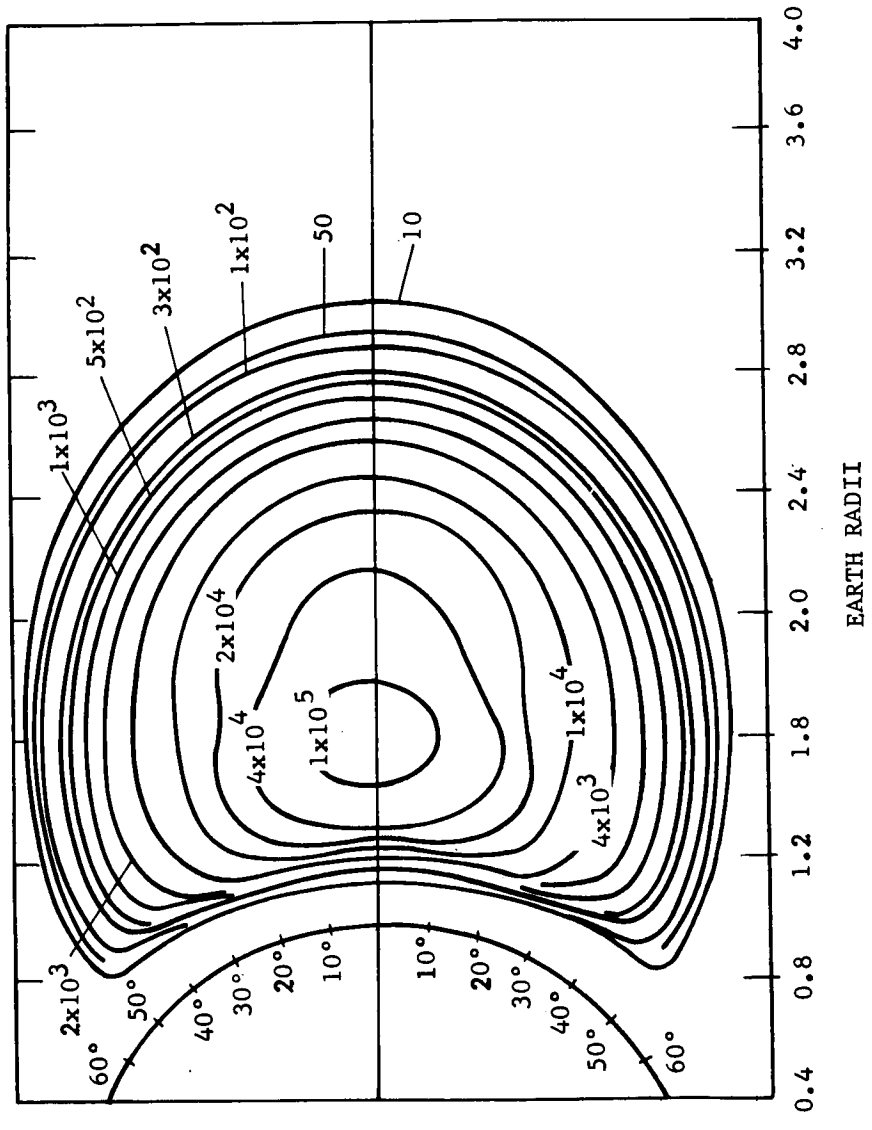


Figure 1-7. THE R- λ FLUX MAP FOR AP 2, SEPTEMBER 1963 (The contours are the omnidirectional flux (protons/cm²-sec) above 15 MeV.)

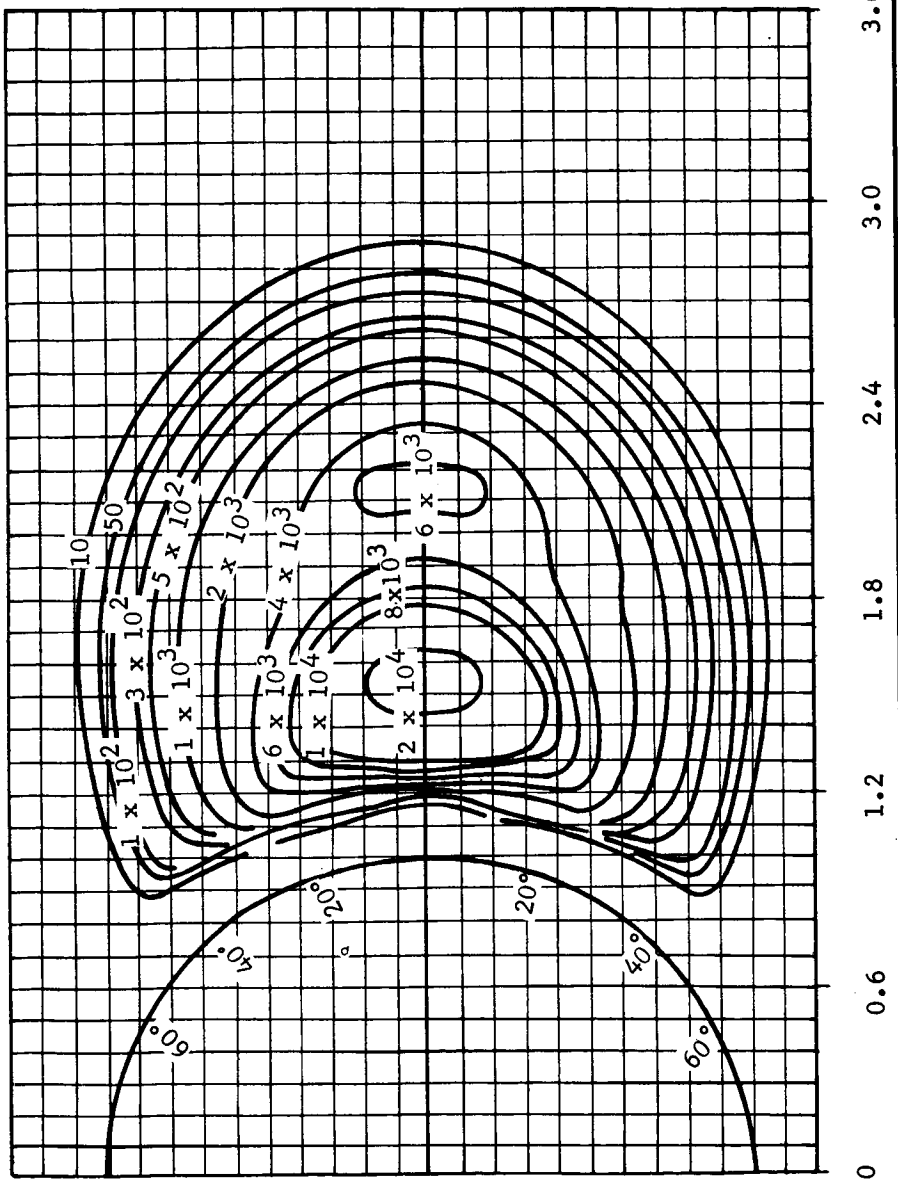


Figure 1-8. THE R- λ FLUX MAP FOR API BEFORE SEPTEMBER 23, 1963
 (The contours are the omnidirectional flux (protons/cm²-sec)
 above 34 MeV.)

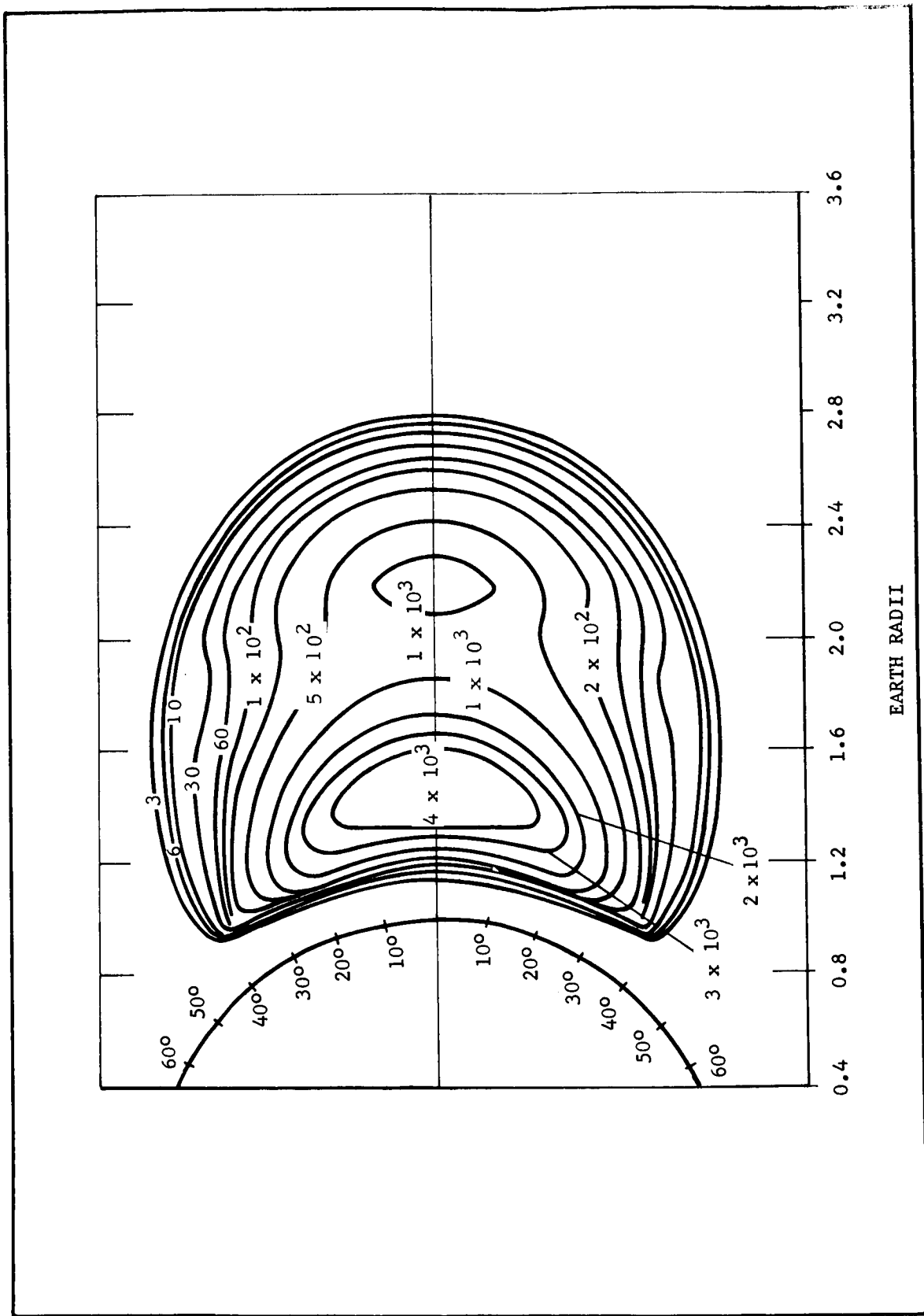
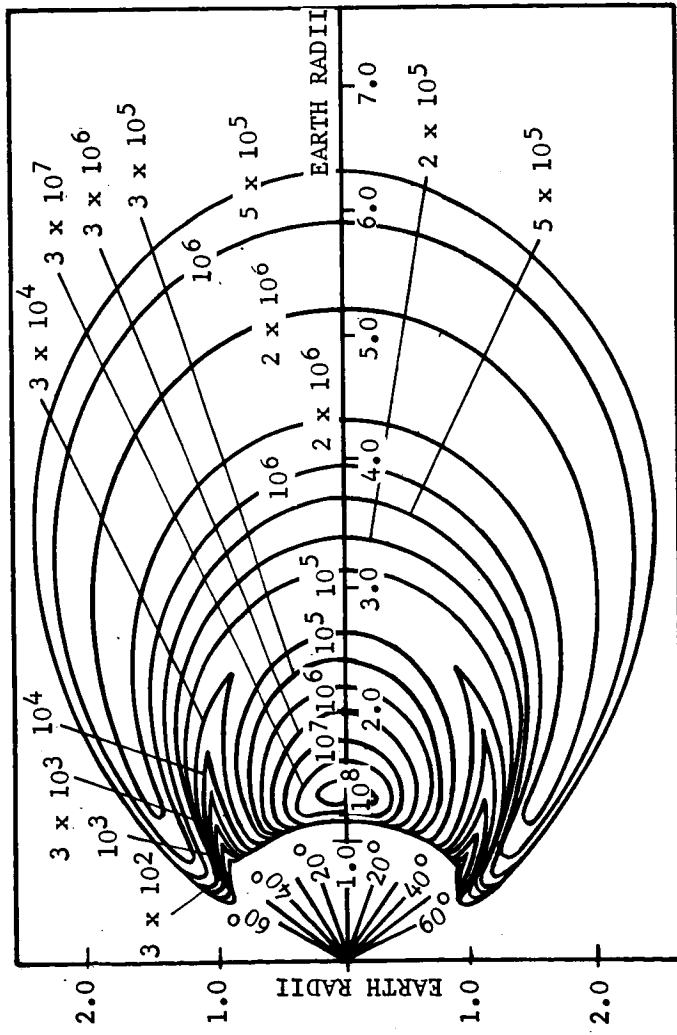


Figure 1-9. THE R- λ FLUX MAP FOR AP3, SEPTEMBER 1963 (The contours are the omnidirectional flux (protons/cm²-sec) above 50 MeV.)

Figure 1-10. THE R- λ FLUX MAP OF THE AE2 ENVIRONMENT



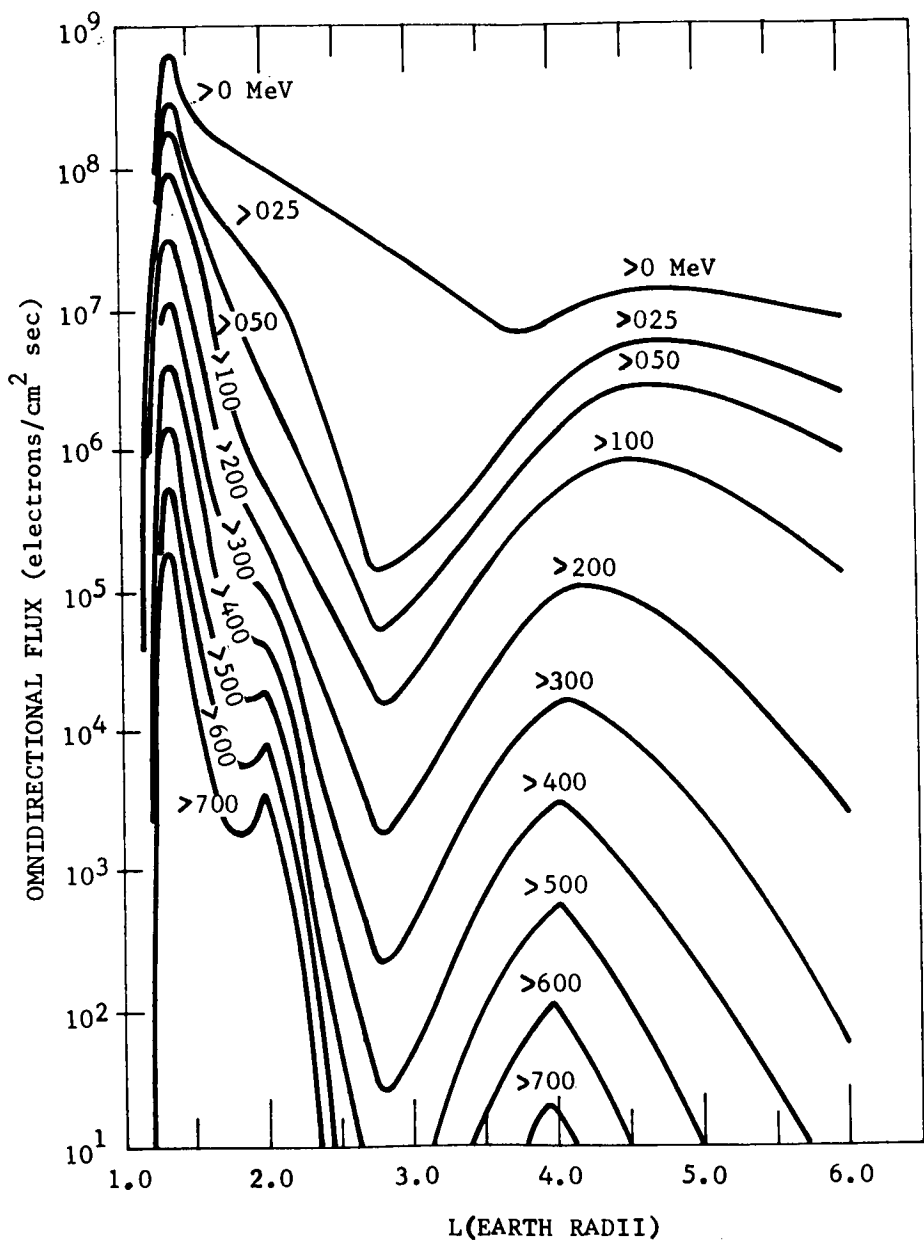


Figure 1-11. ELECTRON OMNIDIRECTIONAL FLUX MAP AE2 (ELECTRONS/CM² SEC) AT THE GEOMAGNETIC EQUATOR

- Integrated yearly rate: $\sim 1.3 \times 10^8$ protons/cm²
- Flux at sunspot minimum: $\sim 2.0 \pm 0.3$ protons/cm² - sec
(isotropic)
- Integrated yearly rate: $\sim 7 \times 10^7$ protons/cm²
- Energy range: 40 MeV to 10^{13} MeV; predominant energy 10^3 - 10^7 MeV

The variation in flux is given in Figure 1-12.

1.4.4 Solar Flares

The probability of the occurrence of various fluxes of particles with energies exceeding 30 MeV is given in Figure 1-13 as a function of mission length.

Solar flares have a composition consisting predominantly of protons. Occasionally the proton-to-alpha-particle ratio may be as low as one, but more likely the ratio will be on the order of 10.

The monthly particle integrated flux is given in Figure 1-14 for solar cycle 19. The dashed curve represents the 10.7 cm solar flux.

The minimum momentum required by a particle to penetrate the geomagnetic field to the Earth's surface is given in Figure 1-15 as a function of geomagnetic latitude.

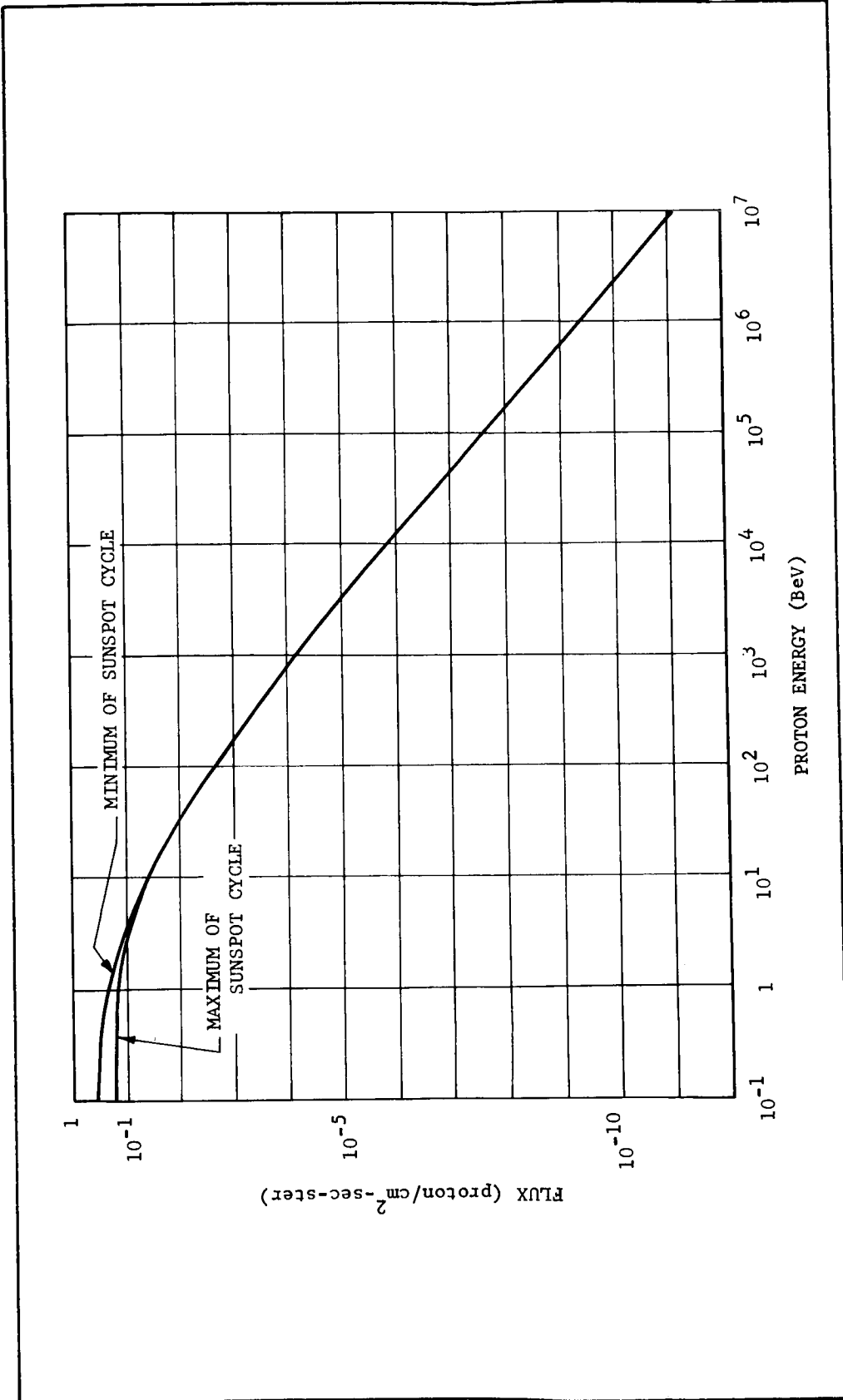


Figure 1-12. INTEGRAL-COSMIC-RAY ENERGY SPECTRUM AT EXTREMES OF THE SUNSPOT CYCLE (Space-probe measurements give a flux value of approximately 0.2 particle/cm²-sec-sterad above about 40 MeV near sunspot maximum; this value should increase by a factor of about 2.5 near sunspot minimum.)

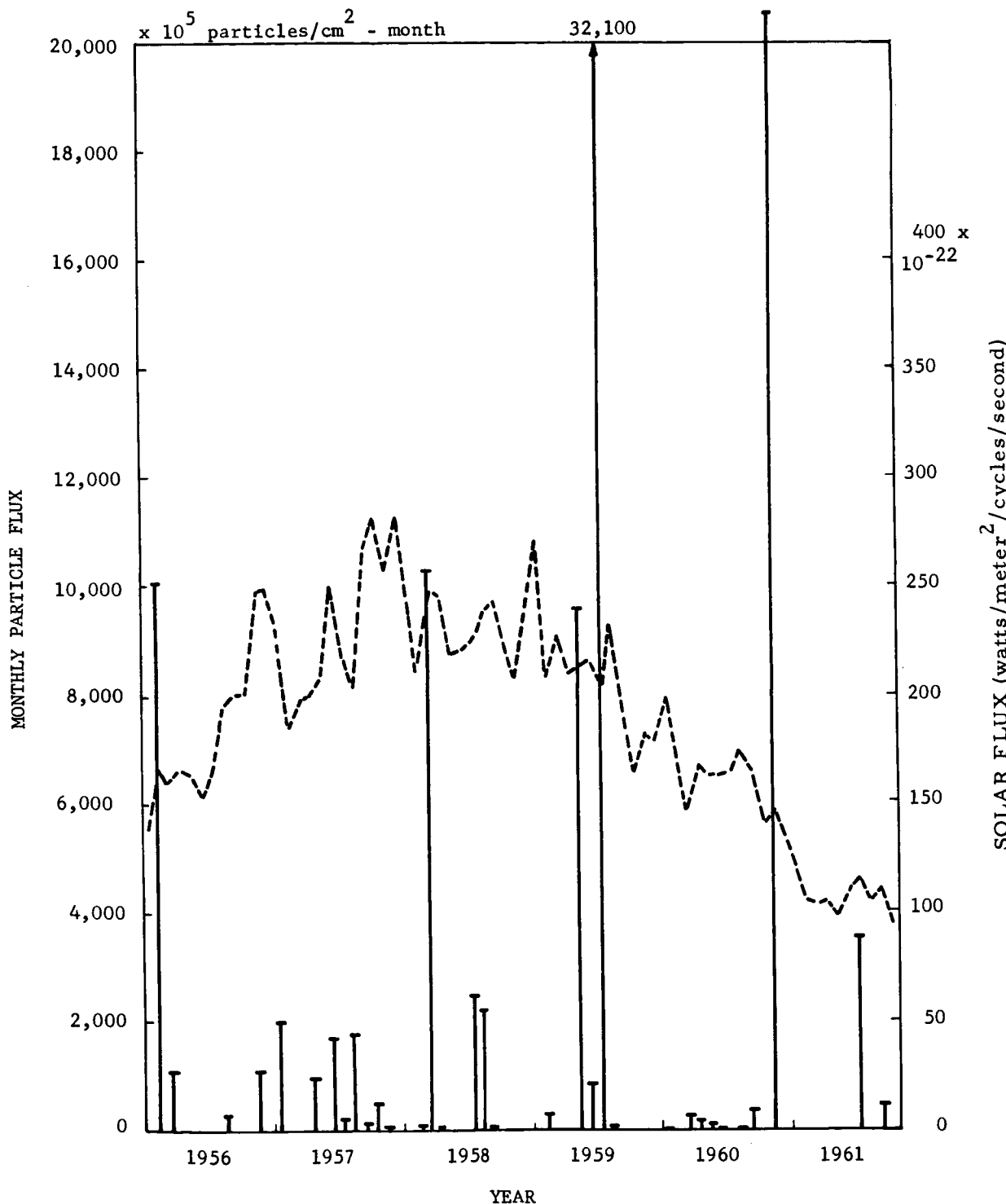


Figure 1-14. FLUX OF PARTICLES WITH ENERGIES EQUAL TO OR GREATER THAN 30 MeV FROM SOLAR FLARES DURING THE LAST SOLAR CYCLE (These are shown as total flux per month of particles with energies equal to or exceeding 30 MeV. The dashed line is the monthly mean value of the solar flux at 2800 Mc/s.)

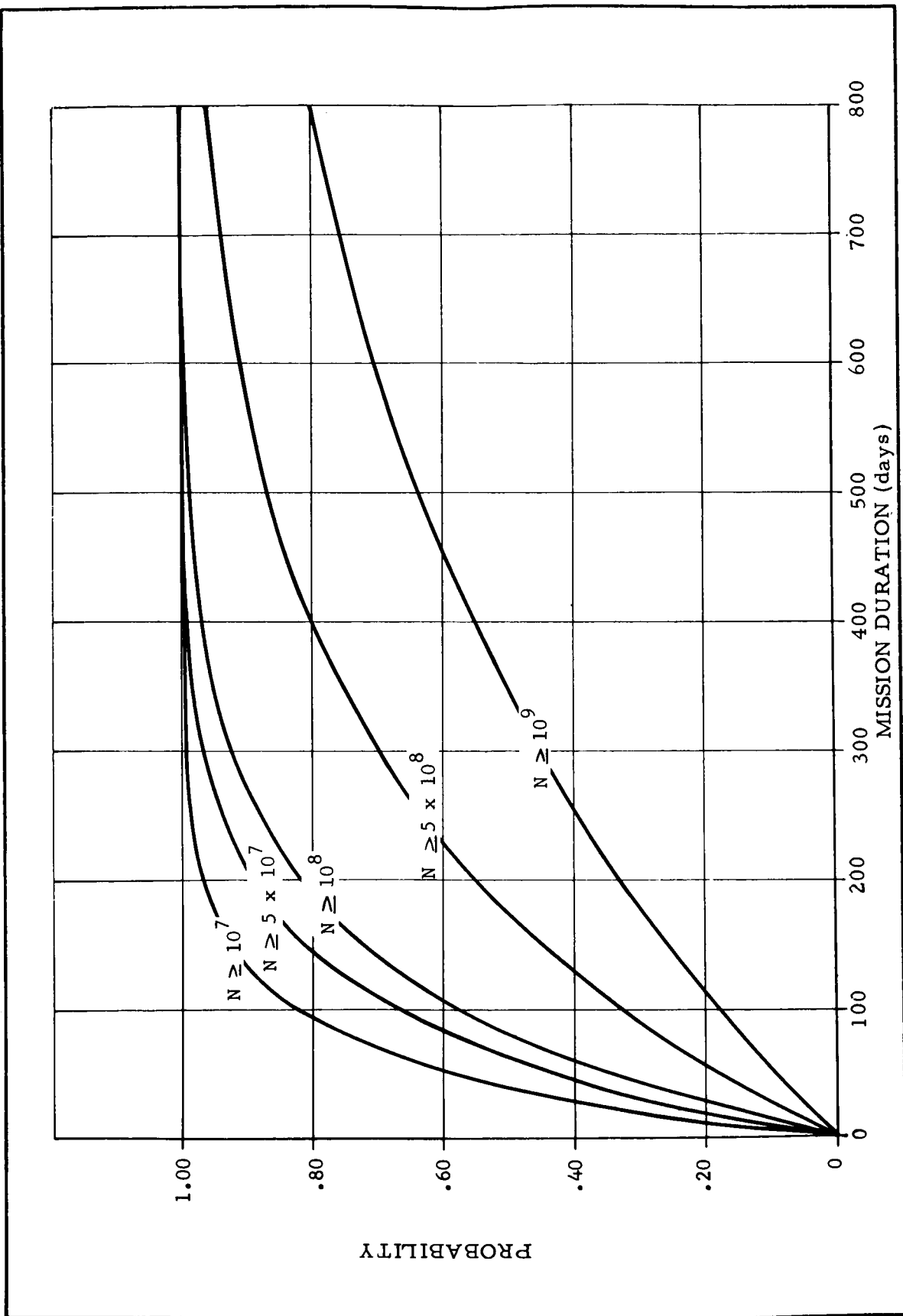


Figure 1-13. PROBABILITY p , IN A MISSION LASTING d DAYS, OF THE OCCURRENCE OF ONE OR MORE SOLAR FLARES WITH FLUX GREATER THAN OR EQUAL TO N WITH ENERGIES GREATER THAN OR EQUAL TO 30 MeV .

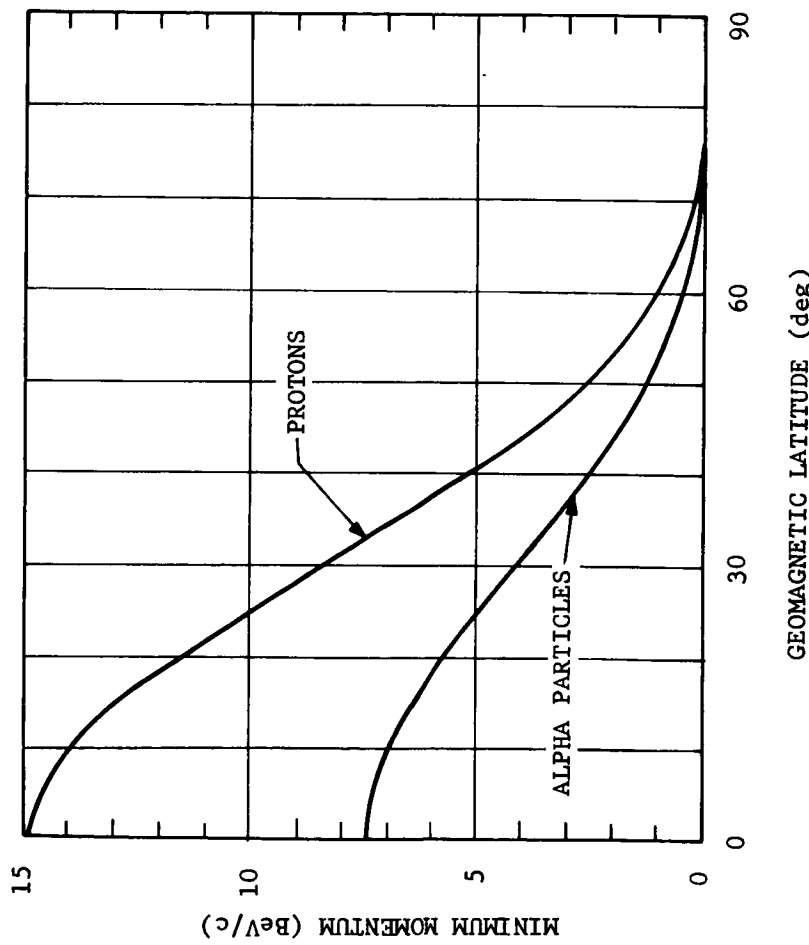


Figure 1-15. GEOMAGNETIC CUT-OFF MOMENTA FOR VERTICALLY INCIDENT PROTONS AND ALPHA PARTICLES AT THE EARTH'S SURFACE FOR VARIOUS GEOMAGNETIC LATITUDES

1.5

GRAVITY

The gravitational potential function is as follows:

$$\Phi(R, \phi) = \frac{GM_E}{R} \left[1 + \frac{J_2 R_E^2}{2R^2} (1 - 3 \sin^2 \phi) + \frac{J_3 R_E^3}{2R^3} (3 - 5 \sin^2 \phi) \sin \phi - \frac{J_4 R_E^4}{8R^4} (3 - 30 \sin^2 \phi + 35 \sin^4 \phi) + \frac{3J_{22} R_E^2}{R^2} \cos^2 \phi \cos 2(\lambda - \lambda_{22}) \right],$$

where

R = radius

ϕ = latitude

$J_2 = 1082.30 (\pm 0.2) \times 10^{-6}$

$J_3 = -2.3 (\pm 0.1) \times 10^{-6}$

$J_4 = -1.8 (\pm .2) \times 10^{-6}$

$J_{22} = 1.9 \times 10^{-6}$

$\lambda_{22} = 21^\circ$ longitude

λ = longitude.

1.6

METEOROIDS

The mass and dimensions of a meteoroid cannot be measured directly because the material is dispersed as it passes

through the atmosphere. These properties must therefore be inferred from the observed luminosity and velocity of the meteor. The brightness of the trail is related to the kinetic energy of the meteoroid. Estimates of the density of meteoroids indicate that for the majority the values lie between 0.01 and 0.7 gm/cm³. Some authorities have adopted a density of 0.44 gm/cm³ for calculational purposes.

Meteoroid models have been formulated which present the variation of incident flux ($F >$) and puncture flux (\emptyset) for asteroidal and cometary particles as a function of heliocentric distance (R). These relationships are as follows:

o Asteroidal Particles

$$\log F > = -15.93 - \log m + 13.15 \log R$$

$$\log \emptyset = -(54/19) (k_t + \log p) - 15.17 + 12.20 \log R$$

o Cometary Particles

$$\log F > = -14.20 - 1.386 (\log m) - 0.0331 (\log m)^2$$

$$+ 0.00051 (\log m)^3 - (3/2) \log R$$

$$\log \emptyset = -13.03 - 3.81 (k_t + \log p) - 0.384 (k_t + \log p)^2 - 0.017 (k_t + \log p)^3 - (93/38) \log R$$

The symbols in the preceding equations are defined as:

$F >$ = mean cumulative influx of meteoroids with mass greater than m, in grams.

ϕ = mean puncture flux for hemispherical exposure
without shielding

m = mass of a meteoroid or projectile in grams

R = distance from the sun in astronomical units

k_t = target material parameter

p = thickness of puncturable target sheet in
centimeters

Hence, the incident flux ($F >$) of the asteroidal particles
is proportional to $R^{13.15}$; and the puncture flux (ϕ) is proportional
to $R^{12.20}$.

A listing of major meteor streams is provided in Table
1-5.

Table 1-5. ORBITAL ELEMENTS FOR MAJOR METEOR STREAMS

Name	Period of Activity	Date Max.	E_{\max}	Ω (deg)	π (deg)	ω (deg)	i (deg)	ϵ	a (a.u.)	q (a.u.)	a (a.u.)	Velocity Heliocentric (km/sec)		Period Years
												a (a.u.)	q (a.u.)	
Quadrantids*	Jan 2-4	Jan 3	8.0	282	92	166	67	0.46	0.97	1.7	4.2	3.9	3.9	13
Lyrid	April 19-22	April 21	.85	30.5	--	210	81	0.88	0.90	---	4.8	4.0	4.0	19.8
η - Aquarid	May 1-8	May 4-6	2.2	45	152	108	162	0.96	0.66	17.95	64	41	41	11
O - Cetid	May 14-23	May 14-23	2.0	238	89	211	34	0.91	0.11	1.3	37	33	33	1.5
Arietid	May 29-June 19	June 6	4.5	77	106	29	21	0.94	0.09	1.6	38	34	34	1.8
ζ - Perseid	June 1-16	June 6	3.0	78	--	59	4±2	0.79	0.35	1.6	29	35	35	2.2
β - Taurids	June 24-July 5	June 28	2.0	276	162±4	246±4	9±4	0.86	0.36	2.5	31	37	37	3.3
δ - Aquarid	July 26-Aug 5	July 28	1.5	305	101±2	156±2	24±5	0.96	0.08	1.8	40	35	35	3.6
Perseid	July 15-Aug 18	Aug 10-14	5.0	142	--	155	114	0.96	0.97	23	60	42	42	109.5
Giacobinid*	Oct 9-10	Oct 10	20	196	--	172	30.8	0.72	0.99	3.5	23	41	41	6.57
Orionid	Oct 15-25	Oct 20-23	1.2	29.3	103	87.8	163	0.92	0.54	6.32	66	41.5	41.5	--
Arietid, Southern	Oct-Oct	Nov 5	1.1	27	150	122	6	0.85	0.30	1.91	28	36	36	2.64
Taurids, Northern	Oct 26-Nov 22	Nov 10	0.4	221	160	308	2.5	0.86	0.31	2.16	29	37	37	3.2
Taurids, Night	Nov	1.0	220	160	300	3	0.86	0.3	2.1	37	37	37	37	3.3
Taurids, Southern	Oct 26-Nov 22	Nov 5	0.9	45	157	112	5.1	0.85	0.36	2.39	28	38	38	3.69
Leonid*	Nov 15-20	Nov 16-17	0.9	234	49	179	162	0.92	0.99	12.8	72	41	41	33.25
Bielids*	Nov 15-Dec 6	Dec 12-13	2.5	250	109	223	13	0.76	0.88	3.6	16	39.5	39.5	6.6
Geminid	Nov 25-Dec 17	Dec 22	4.0	261	--	324	24	0.90	0.14	1.4	35	35	35	1.7
Ursids	Dec 20-24	Dec 22	2.5	270	--	210	5.3	1.0	0.92	--	37	42	42	--

*Periodic streams

SECTION II
INTERPLANETARY ENVIRONMENT
BETWEEN EARTH AND MARS

2.1 ATMOSPHERE

2.1.1 Kinetic Gas Temperature

The kinetic gas temperature is approximately 2×10^5 °K at the Earth's mean orbital distance and approximately 1.9×10^5 °K at the Martian mean orbital distance (1.52 A.U.).

2.1.2 Gas Pressure

Gas pressure between the orbits of the Earth and Mars varies with solar activity. During quiet solar conditions it is approximately 10^{-10} dynes/cm².

2.1.3 Density

Density, like pressure, also varies with solar activity. The gas density of interplanetary matter is approximately 10^{-23} gm/cm³. The electron density decreases with an increase in distance from the solar surface. Figure 2-1 shows the electron density versus the distance above the solar limb in the equatorial plane at about the time of sunspot minimum. The composition of the interplanetary atmosphere is primarily hydrogen, protons, helium and alpha particles.

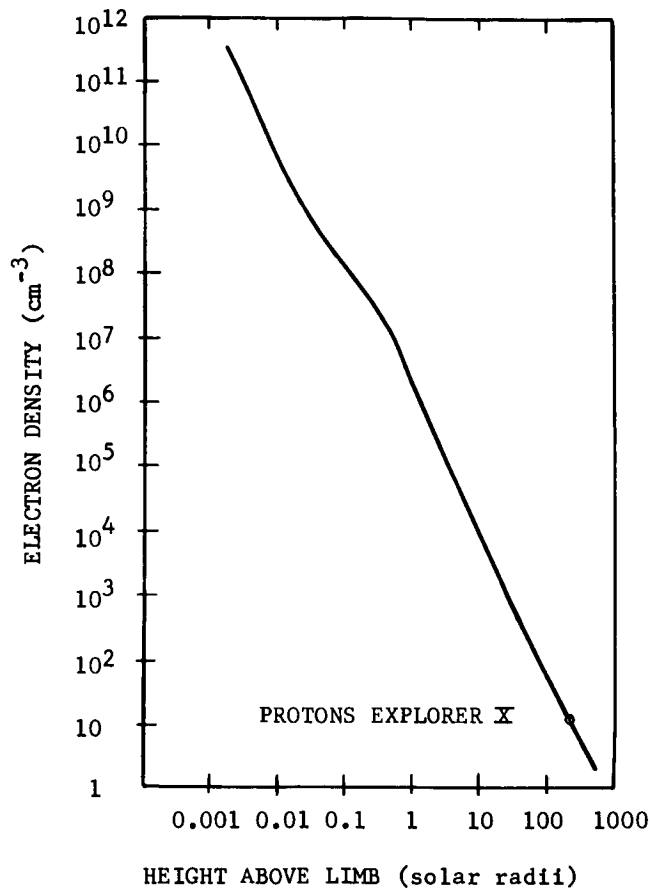


Figure 2-1. ELECTRON DENSITY AS A FUNCTION OF DISTANCE ABOVE THE SOLAR LIMB IN THE EQUATORIAL PLANE AT ABOUT THE TIME OF SUNSPOT MINIMUM

2.2 SOLAR THERMAL RADIATION

Using the solar constant at 1.0 A.U. as 1400 watts/m^2 , and incorporating the inverse square law of radiation, the radiation in space at a distance R , measured in AU's, will be $1400 (1/R)^2 \text{ watts/m}^2$.

Table 2-1 shows the variation of solar constant with solar distance.

Table 2-1 VARIATION OF SOLAR CONSTANT
WITH SOLAR DISTANCE

Solar Distance (A.U.)	Solar Constant (watts/m ²)	Solar Distance (A.U.)	Solar Constant (watts/m ²)
0.5	5600	1.2	972
0.6	3889	1.3	828
0.7	2857	1.4	714
0.8	2187	1.5	622
0.9	1728	1.6	547
1.0	1400	1.7	484
1.1	1157	1.75	457

- Brightness of the sun: $200,000 \text{ candles/cm}^2$

- Solar illumination: $13.4 R^{-2} \text{ lumens/cm}^2$

$$\text{or } 1.34 \times 10^5 R^{-2} \text{ lumens/m}^2$$

where R = distance from sun (A.U.).

The principal magnetic field in space from 1.0 to 1.5 A.U. solar distance is that of the sun as carried by the solar plasmas. The strength of the solar interplanetary magnetic field at 1.0 A.U. is about 5 gammas. The strength of the field depends upon solar activity, with maximum field strength at maximum solar activity. Fluctuations of one or two orders of magnitude may occur depending upon solar activity.

Near the orbit of Mars the average interplanetary magnetic field could be less than that at 1.0 A.U. or less than 5 gammas.

The interplanetary field appears to be directed along the classical Archimedean spiral from the sun as described by Parker, but the remote possibility of a distorted solar dipole field should not be excluded.

2.4 GALACTIC COSMIC RADIATION

- Composition: ~ 85% proton (H^+)
~ 14% alpha particles (He^{++})
~ 1% nuclei of elements Li → Fe
(in approximate cosmic abundance)
- Flux at sunspot maximum: ~ 4 protons/cm² - sec
(isotropic)

- Integrated yearly rate: $\sim 1.3 \times 10^8$ protons/cm²
- Flux at sunspot minimum: $\sim 2.0 \pm 0.3$ protons/cm² sec (isotropic)
- Integrated yearly rate: $\sim 7 \times 10^7$ protons/cm²
- Energy range: 40 MeV to 10^{13} MeV; predominant energy $10^3 - 10^7$ MeV

2.5 SOLAR COSMIC RADIATION

2.5.1 Solar High Energy Particle Radiation

- Composition: Predominantly of protons (H^+) and alpha particles (He^{++})
- Integrated yearly flux at 1 A.U.:

Energy > 30 MeV, $J \approx 6 \times 10^9$ protons/cm² near solar maximum

$J \approx 1 \times 10^9$ protons/cm² near solar minimum

Energy > 100 MeV, $J \approx 1 \times 10^9$ protons/cm² near solar maximum

$J \approx 1 \times 10^8$ protons/cm² near solar minimum

The accurate description of this radiation at space distance other than 1 A.U. has not been established, but the inverse

square law can be used for rough estimations.

2. 5. 2 Solar Flares

A solar flare is a bright eruption from the sun's chromosphere associated with the release of large amounts of energy. The larger flares eject charged particles into the interplanetary medium. Those particles captured by the Earth produce a polar cap absorption event. In some cases a flare produces particles with energy of 1 to 50 GeV which produce ground level events on the Earth.

There is an apparent higher probability that solar proton events, recorded at the Earth, will occur near the equinoxes (the times when the sun crosses the Earth's equator) than during the months of June or December.

During a period of high solar activity, the probability, p , of encountering a flare with total integrated flux, N , with energies greater than 30 MeV in one day is given in Figure 2-2, where n_f is the number of occurrences of flares whose individual total integrated flux exceeded the largest recorded flare, and n_t is the time frame over which the flares were recorded.

2. 5. 2. 1 Model Time Integrated Spectral Distribution.

$$N(>P) = N_0 \exp(-P/P_0),$$

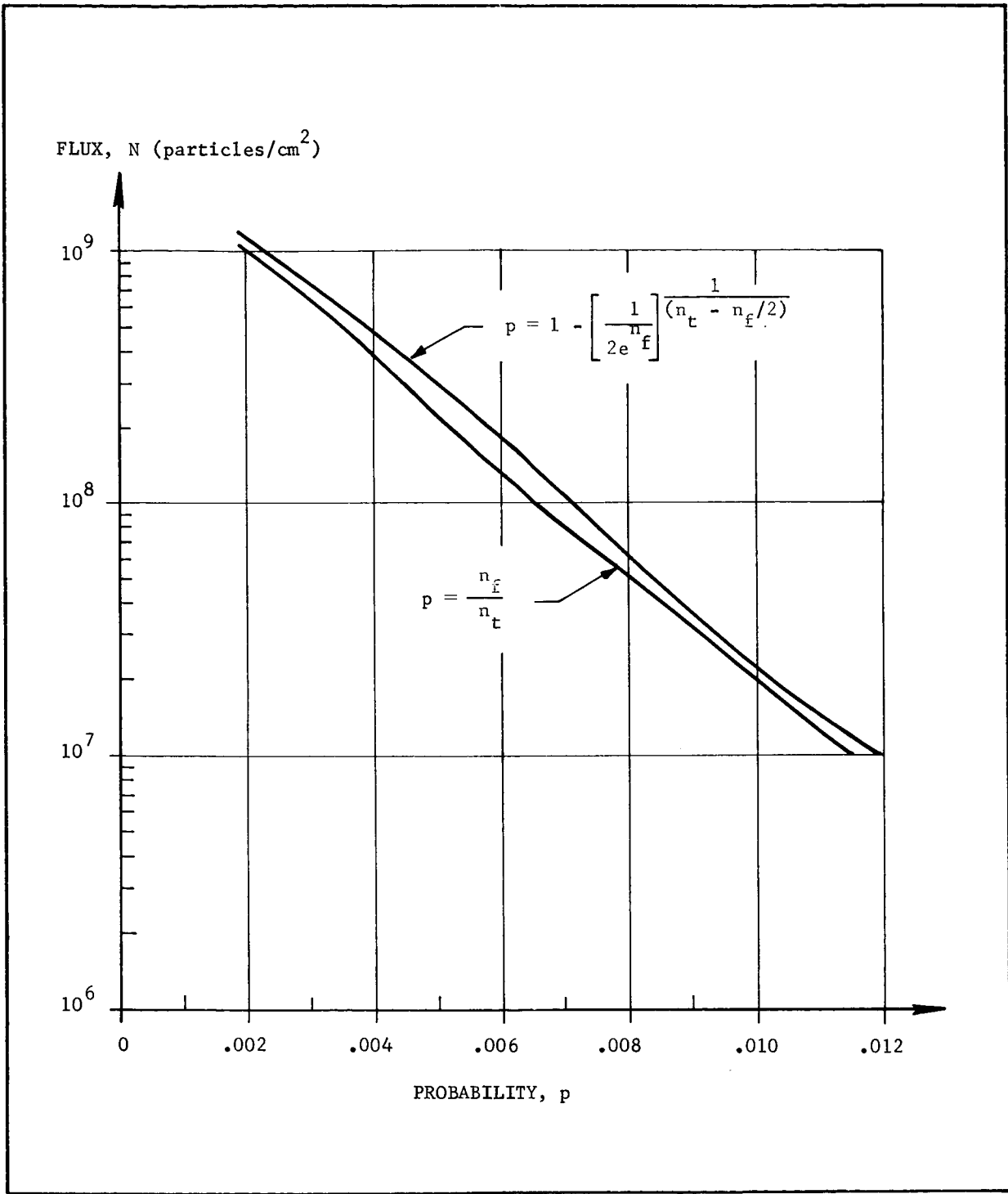


Figure 2-2. THE PROBABILITY, p , OF THE OCCURRENCE OF A FLARE WHOSE FLUX IS EQUAL TO OR GREATER THAN N , AND WHOSE INDIVIDUAL PARTICLE ENERGIES ARE EQUAL TO OR GREATER THAN 30 MeV

where

$N = \text{protons/cm}^2$ having rigidity greater than P

$P = \text{rigidity, or momentum per unit charge, in volts}$

$P_o = 97 \text{ MeV}$, a value typical for large events

$N_o = \text{total intensity of event (particles/cm}^2\text{)}$

$$P = \frac{1}{eZ} \left(T^2 + 2Tm_o c^2 \right)^{1/2}$$

where

$eZ = \text{nuclear charge}$

$T = \text{proton energy (MeV)}$

$m_o c^2 = \text{proton rest energy} = 938.2 \text{ MeV for protons}$

$3727.1 \text{ MeV for alpha}$

particles

P_o is evaluated for energies $T \geq 10 \text{ MeV}$. Below 10 MeV,

the spectrum may be described by the expression: $N(>T) = N_o T^{-n}$,

with n approximately equal to 1.2.

2.5.2.2 Solar Particle Events Near the Earth. The integral spectrum near the Earth is given by

$$N(>P) = N_o e^{-P/P_o}, \quad P \geq P_c$$

$$N(>P) = N_o e^{-P_c/P_o}, \quad P \leq P_c$$

$P_c = \text{cut-off rigidity.}$

(For all rigidities below P_c , the intensity is zero.) The cut-off rigidity is given by

$$P_c = \frac{2.5 \times 10^9}{r^2} \left(\frac{2 + \cos^3 \lambda - 2(1 + \cos^3 \lambda)^{1/2}}{\cos^2 \lambda} \right)$$

r = geocentric radius (km)

λ = geomagnetic latitude.

For the probability (p) of encountering more than N protons/cm² with rigidity (P) greater than 0.235 Bv for various mission lengths, refer to Table 2-2. Although the rate of change of the number of protons/cm² with solar distance is unknown, the tabulated values given for 0.5 to 1.75 A.U. may be used as a guideline.

2.5.3 Solar Wind

The solar wind is an outward flux of material from the corona of the sun.

- Mean density: 0.5 A.U. \approx 20 protons/cc
1.0 A.U. \approx 5 protons/cc
1.75 A.U. \approx 2 protons/cc
- Mean flux: 0.5 A.U. \approx 8×10^8 protons/cm²/sec
1.0 A.U. \approx 2×10^8 protons/cm²/sec
1.75 A.U. \approx 10^8 protons/cm²/sec

- Mean velocity of solar wind from 0.5 A.U. to 1.75

A.U. = 450-500 km/sec.

Table 2-2. PROBABILITY OF PARTICLE ENCOUNTER VS MISSION LENGTH

Mission length, weeks	Probability, p			
	0.50	0.10	0.01	0.001
	N, protons/cm ²			
2	-	5.0×10^7	2.0×10^9	1.7×10^{10}
4	-	2.0×10^8	4.5×10^9	3.3×10^{10}
8	1.3×10^7	7.2×10^8	9.0×10^9	5.6×10^{10}
12	4.5×10^7	1.3×10^9	1.5×10^{10}	8.0×10^{10}
20	1.5×10^8	2.4×10^9	2.2×10^{10}	1.1×10^{11}
30	3.0×10^8	3.9×10^9	3.0×10^{10}	1.4×10^{11}
40	5.0×10^8	5.0×10^9	3.3×10^{10}	1.5×10^{11}
50	7.0×10^8	5.9×10^9	3.5×10^{10}	1.6×10^{11}
60	1.0×10^9	6.2×10^9	3.7×10^{10}	1.6×10^{11}
80	1.6×10^9	7.2×10^9	3.9×10^{10}	1.7×10^{11}
100	2.0×10^9	8.0×10^9	4.0×10^{10}	1.7×10^{11}

2.6 SOLAR RADIATION PRESSURE

- Pressure at 1.0 A.U.: For 100 percent reflecting

$$\text{body} = 9 \times 10^{-5} \text{ dyne/cm}^2$$

$$\text{For black body} = 4.5 \times 10^{-5} \text{ dyne/cm}^2.$$

Radiation pressure variation with solar distance

follows the relation:

$$P = I/c \text{ for black body}$$

$$P = 2I/c \text{ for 100 percent reflecting body}$$

where

$$P = \text{radiation pressure}$$

I = intensity of radiation at specified solar distance

c = speed of light.

- Pressure at 1.52 A.U.: For 100 percent reflecting

$$\text{body} = 4 \times 10^{-5} \text{ dynes/cm}^2$$

$$\text{For black body} = 2.0 \times 10^{-5}$$

$$\text{dynes/cm}^2.$$

2.7 METEOROIDS

Table 1-5 in Section I presents the major meteor streams for the interplanetary environment between Earth and Mars. The cometary meteoroid flux model and the asteroidal meteoroid flux model as presented in Paragraph 1.6 may be utilized for this environment, using appropriate values for distance from the sun.

SECTION III
MARTIAN ENVIRONMENT
SURFACE TO 10 MARS RADII

3.1 CLIMATE

3.1.1 Surface Temperatures

Seasonal isotherm maps of the Martian daytime ground-surface temperatures are presented in Figures 3-1, -2 and -3. Seasonal differences noted in these maps are due primarily to the eccentricity of the Mars orbit (Figure 3-4). Since the southern summer solstice occurs near perigee and the northern summer solstice occurs near apogee, the warm season in the southern hemisphere is shorter and hotter than in the northern hemisphere. The length of seasons and the heliocentric longitudes are given in Table 3-1.

Table 3-1. LENGTH OF SEASONS FOR VARIOUS HELIOCENTRIC LONGITUDES

HELIOPHILIC LONGITUDE	NORTHERN HEMISPHERE	SOUTHERN HEMISPHERE	DURATION	
			Earth Day	Mars Days
87-177	Spring	Autumn	199	194
177-267	Summer	Winter	182	177
267-357	Autumn	Spring	146	142
357-87	Winter	Summer	160	156

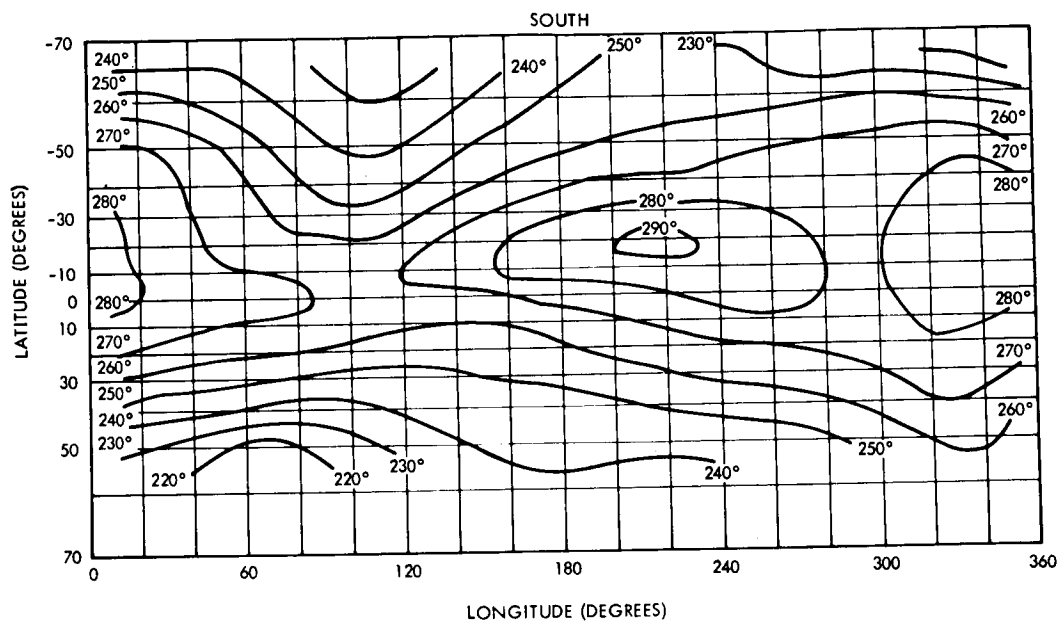


Figure 3-1. SEASONAL ISOTHERMS, SOUTHERN HEMISPHERE SUMMER

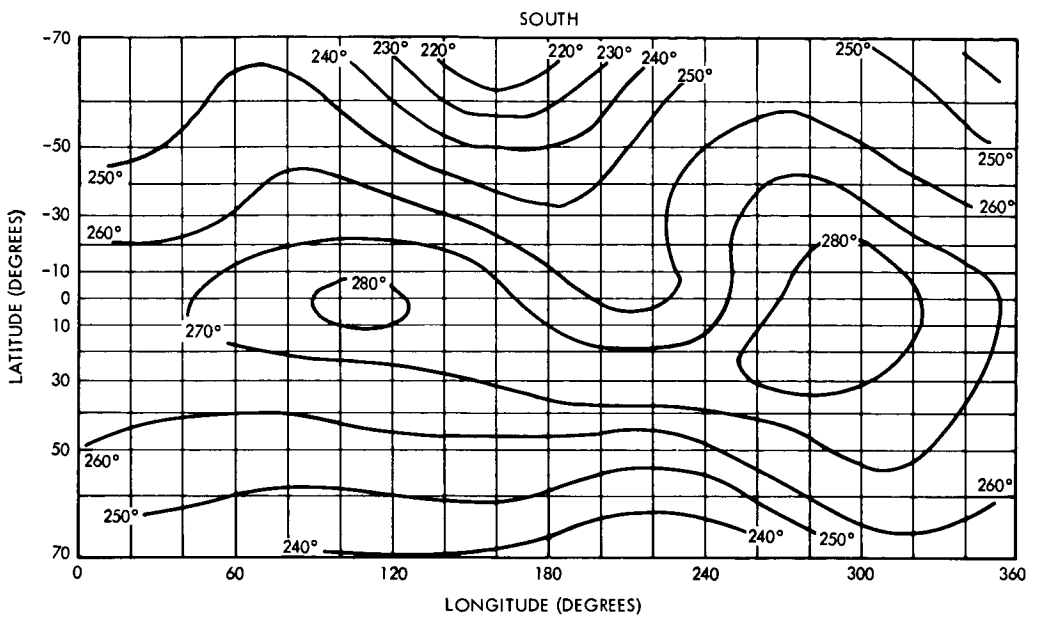


Figure 3-2. SEASONAL ISOTHERMS, SOUTHERN HEMISPHERE FALL

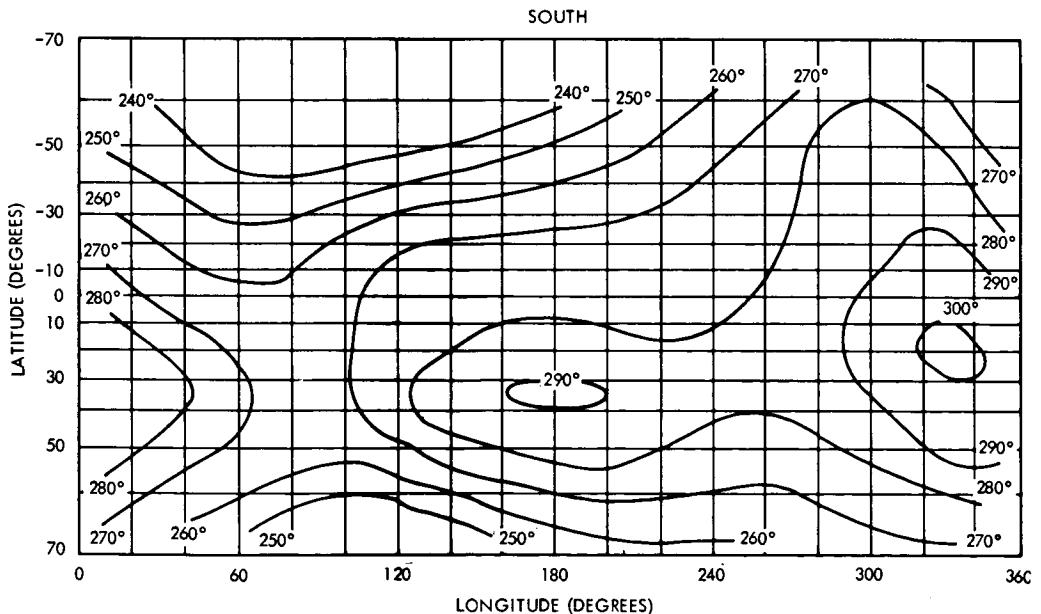


Figure 3-3. SEASONAL ISOTHERMS, SOUTHERN HEMISPHERE WINTER

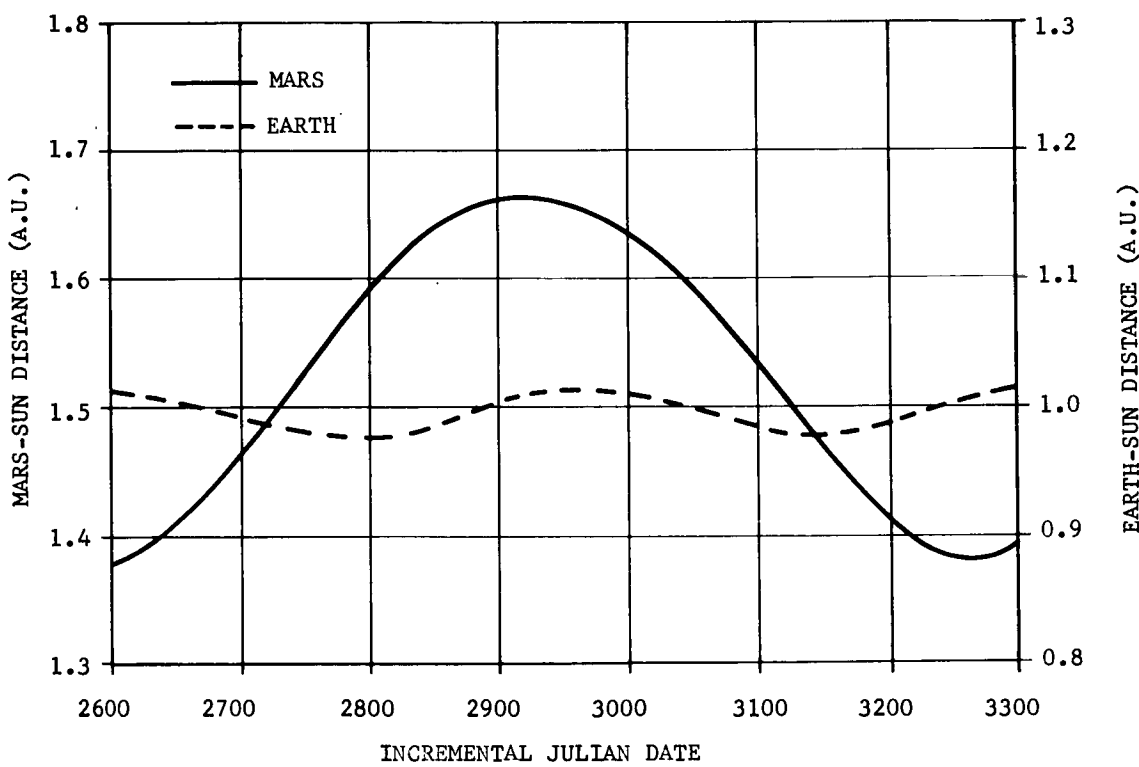


Figure 3-4. VARIATIONS IN SUN-MARS AND SUN-EARTH DISTANCES

The diurnal variations in the ground-surface temperature and atmospheric temperature near the surface are given in Figure 3-5. It is immediately obvious that the seasonal and diurnal variations in the vertical temperature gradient are very large, as indicated in Figure 3-6. The temperature of 260° K indicated in Figure 3-6 is taken to represent the mean temperature. The tropopause altitude "h" is expected to vary from a few meters to 14 km. The principal point of interest in this figure, however, is the extreme variation in the vertical temperature gradients of the "a" and "b" profiles. It should also be noted that the atmospheric temperature may be either warmer or colder than the ground-surface temperature.

3.1.2 Observed Seasonal Changes

The variation of the polar caps is one of the most prominent seasonal changes noted on Mars. The polar caps vary greatly in size; the longer, colder winter in the southern hemisphere produces a polar cap $\sim 70^{\circ}$ in breadth while the shorter, warmer winter in the northern hemisphere produces a cap $\sim 53^{\circ}$ in breadth, approximately three quarters of the size of the southern cap. As a cap recedes, a dark bluish band follows the edge of the retreating polar cap border; the band around the southern cap is the most pronounced. The light coming from these bands has been found to be polarized indicating that it is being reflected from a smooth surface

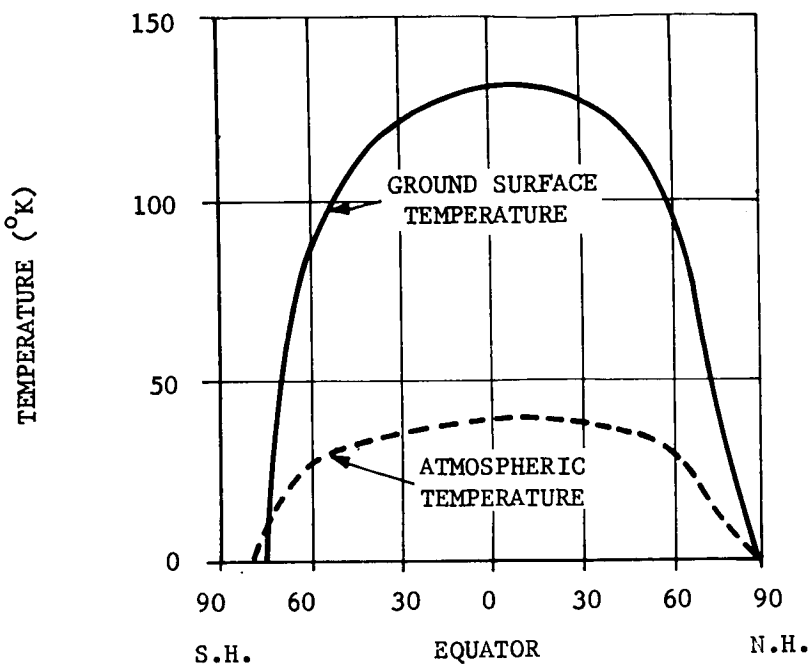


Figure 3-5. DIURNAL VARIATION IN THE MARTIAN ATMOSPHERIC AND GROUND TEMPERATURE

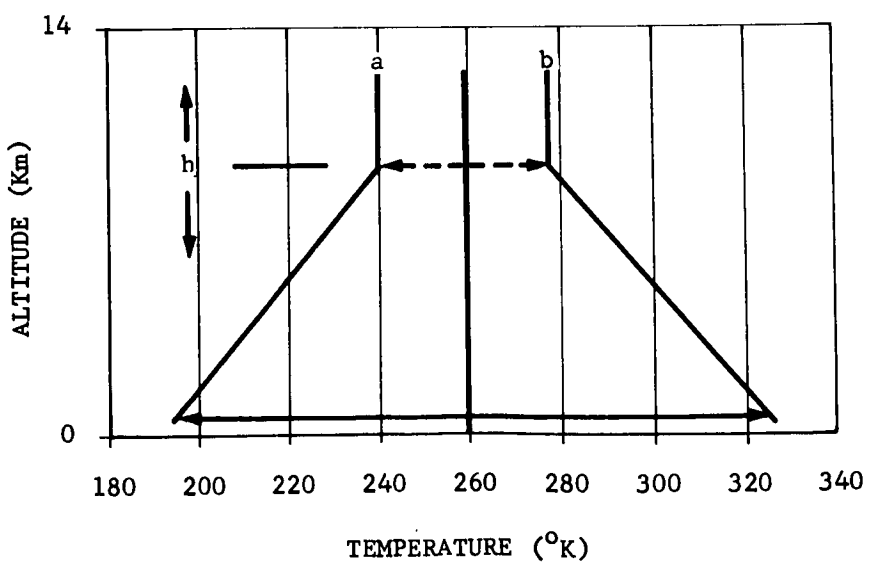


Figure 3-6. DIURNAL VARIATION IN THE MARTIAN TEMPERATURE PROFILE

which, in turn, suggests the presence of water. The regularly observed fluctuations of the polar caps with the Martian seasons infer an atmospheric circulation system and the transport of atmospheric moisture as the mechanism responsible for the deposition and recession of the polar caps as a function of solar energy.

The principal characteristics of the other seasonal changes can be summarized as follows:

- Dark areas darken in the spring and summer and become relatively light again in the autumn and winter.
- Some light areas become dark in the spring and summer and become light again in the autumn and winter. An outstanding example is Pandorae Fretum.
- Seasonal changes are first observed at the edge of the polar caps during the spring of both hemispheres. As the polar cap recedes, the darkening effect spreads toward the equator and finally, during the summer, crosses into the other hemisphere. It has been calculated that this darkening effect in the southern hemisphere spreads at an average rate of 28 miles per day. The rate of spreading is greater in the southern hemisphere than in the northern hemisphere.

3.2 ATMOSPHERE

3.2.1 Temperature

The temperature versus height profiles illustrated in Figure 3.7 have been idealized to represent the minimum (profile D), mean (profile E), and maximum (profile F) temperature profiles expected to exist in the Mars atmosphere.

Geopotential Height (km)

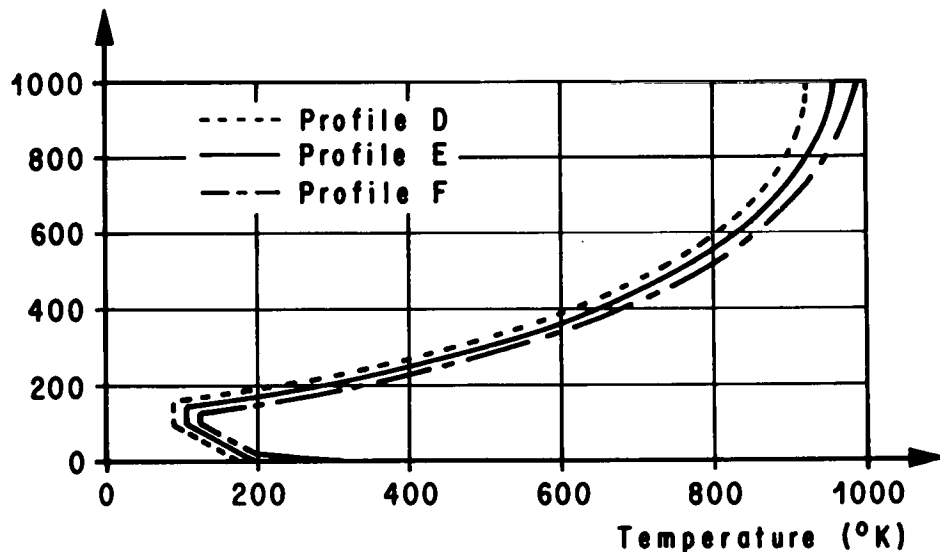


FIG. 3-7. IDEALIZED TEMPERATURE PROFILES

The lower portion of these profiles (0-300 km) are based upon a very detailed analysis of the Mariner IV data as interpreted by various investigators and theoretical heat-budget computations of other investigators. In developing the 300 - 1,000 km extensions to these profiles, consideration was given to the escape velocities of the various constituents that are thought to exist in the Martian upper atmosphere.

3.2.2

Composition and Molecular Weight

The Mars atmosphere is thought to be primarily carbon dioxide with the possibility of small amounts of nitrogen, argon, and water vapor. It is also suspected that the upper atmosphere is under constant bombardment by interplanetary space plasma causing the constituents of the upper atmosphere to become mixed with hydrogen and helium from outer space. This mixing of the Martian atmospheric constituents with interplanetary plasma could possibly occur as low as 300 km altitude. A very extensive review of related literature and a detailed analysis of the average and escape velocities of the constituents in the Mars atmosphere have generated the three molecular weight profiles illustrated in Figure 3-8. These profiles have been idealized to represent the maximum (profile A), mean (profile B), and minimum (profile C) molecular weight profiles and are based upon lower atmosphere compositions of 100% CO₂, 75% CO₂ plus 25% N₂, and 48.8% CO₂ plus 51.2% N₂ respectively.

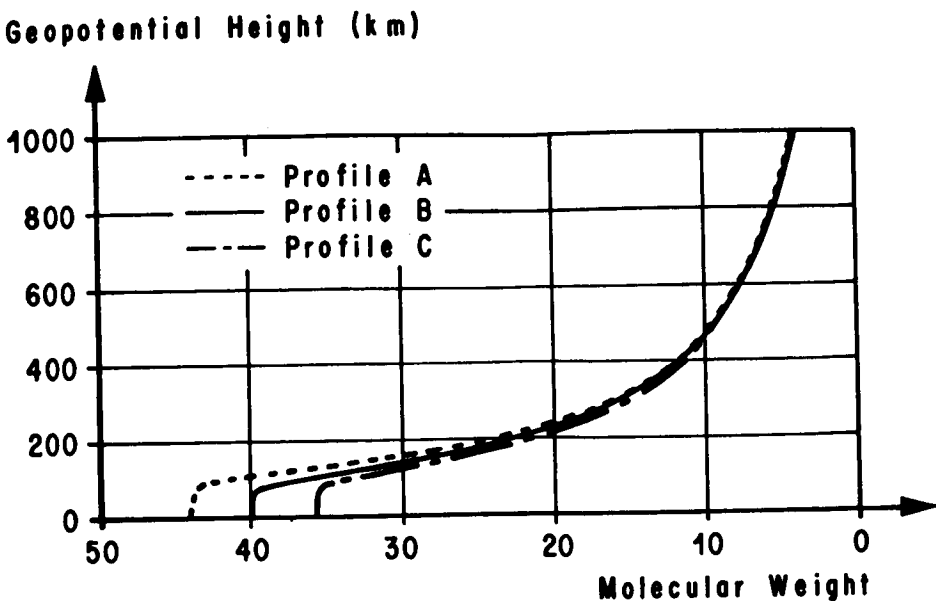


FIG. 3-8. IDEALIZED MOLECULAR WEIGHT PROFILES

3.2.3 Surface Pressure

A detailed review of literature concerning Martian surface pressure values that have been derived from observations of the photographic spectrum of Mars indicates the surface pressure may vary from 4 to 15 ± 5 mb. This range in pressure is further supported by interpretations of Mariner IV data.

3.2.4 Model Atmospheres

Under the assumptions of hydrostatic equilibrium and a perfect gas law relationship among the thermodynamic quantities, a model atmosphere may be generated from a given temperature profile,

molecular weight profile and surface pressure. Three such models have been developed by this technique that define the mean atmosphere and the 99% confidence envelope for Mars. These models were generated from the following criteria:

Mean Model

1. Temperature - Profile E (Fig. 3-7)
2. Molecular weight - Profile B (Fig. 3-8)
3. Surface pressure - 8.0 mb

99% Confidence Envelope

(Minimum model)

1. Temperature - Profile D (Fig. 3-7)
2. Molecular weight - Profile A (Fig. 3-8)
3. Surface Pressure - 4.0 mb

(Maximum model)

1. Temperature - Profile F (Fig. 3-7)
2. Molecular weight - Profile C (Fig. 3-8)
3. Surface pressure - 10.0 mb

3.2.5

Computed Quantities

The various computed quantities of the three model atmospheres are tabulated in Table 3-2 and given as graphic illustrations in Figures 3-9 through 3-20.

3.2.6 Martian Winds

Little is known concerning the instantaneous wind speed on Mars, but the continuous surface and peak surface winds are listed in Table 3-3. It is suspected, however, that the peak surface wind speed on Mars may be as great as 143 m/sec.

3.2.7 Clouds in the Martian Atmosphere

A summary of the Martian clouds that have been observed is given in Table 3-4.

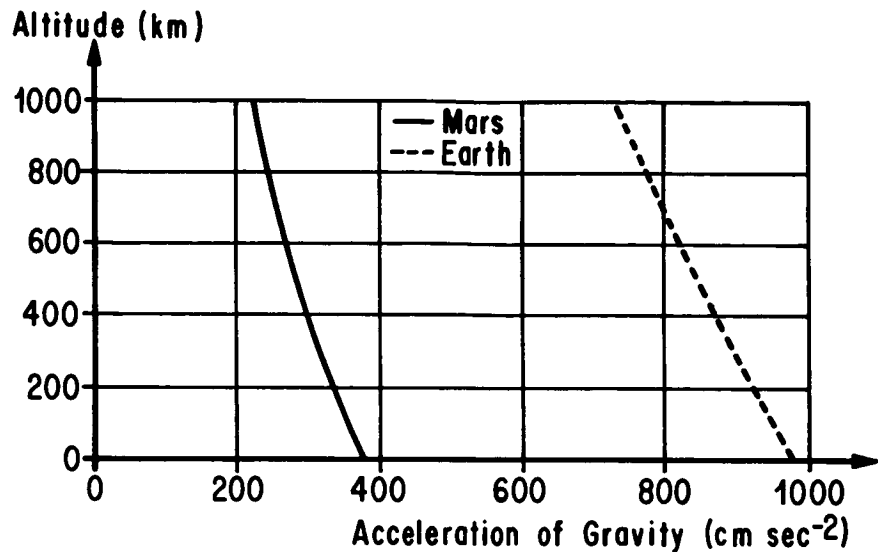


FIG. 3-9. ACCELERATION OF GRAVITY
ON MARS AND EARTH
VERSUS ALTITUDE

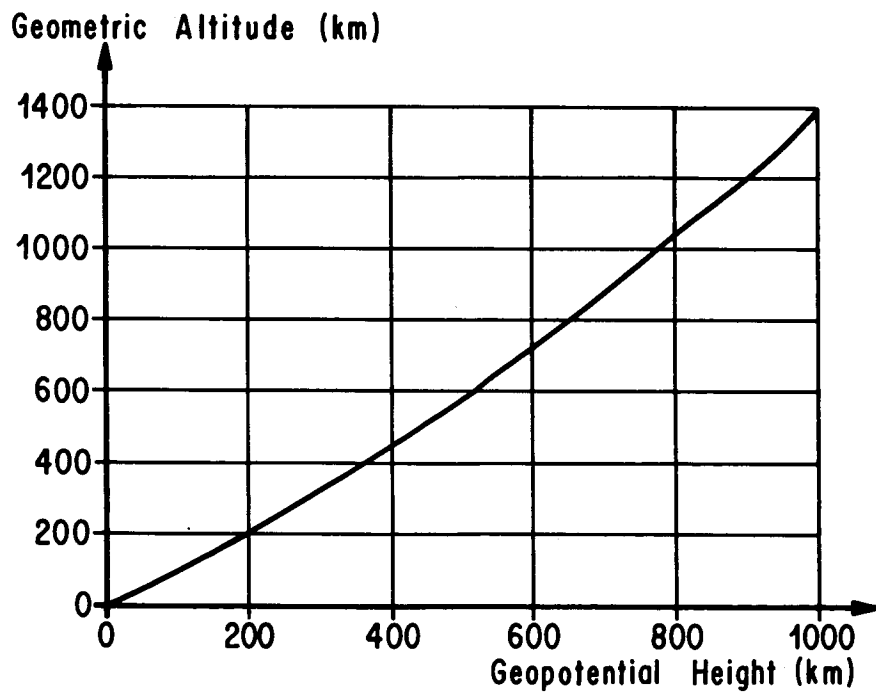


FIG. 3-10. GEOPOTENTIAL HEIGHT VERSUS
GEOMETRIC ALTITUDE ON MARS

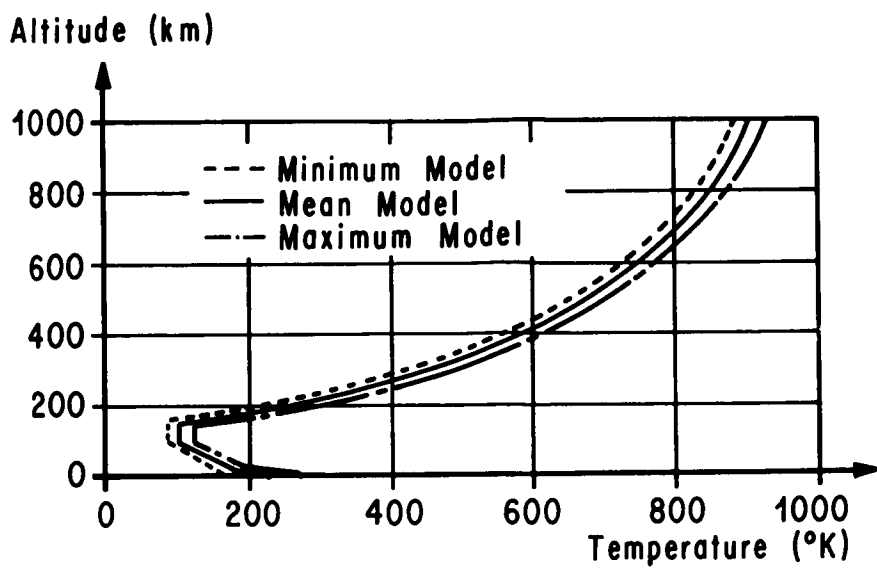


FIG. 3-11. KINETIC TEMPERATURE

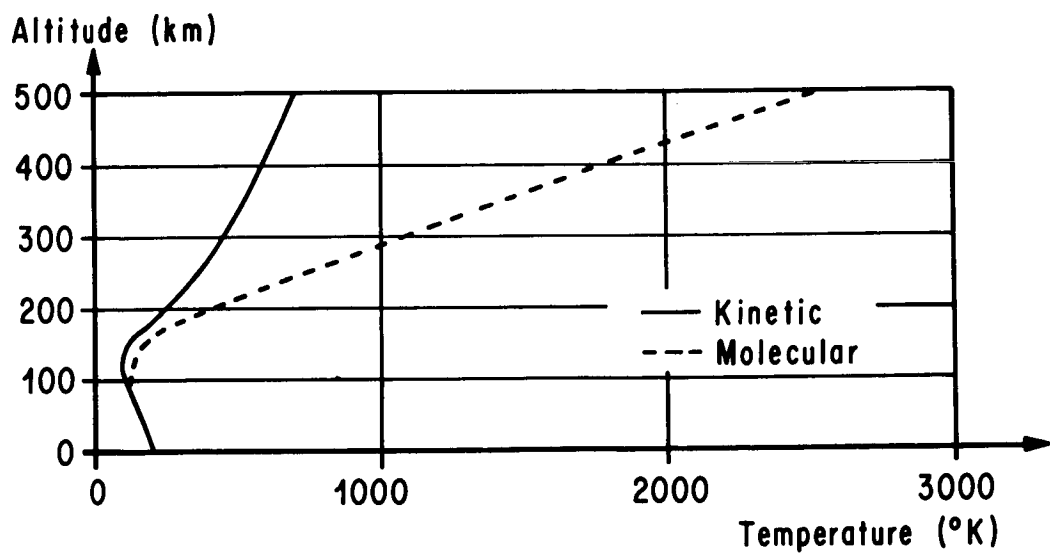


FIG. 3-12. COMPARISON OF
MEAN KINETIC AND MOLECULAR TEMPERATURES

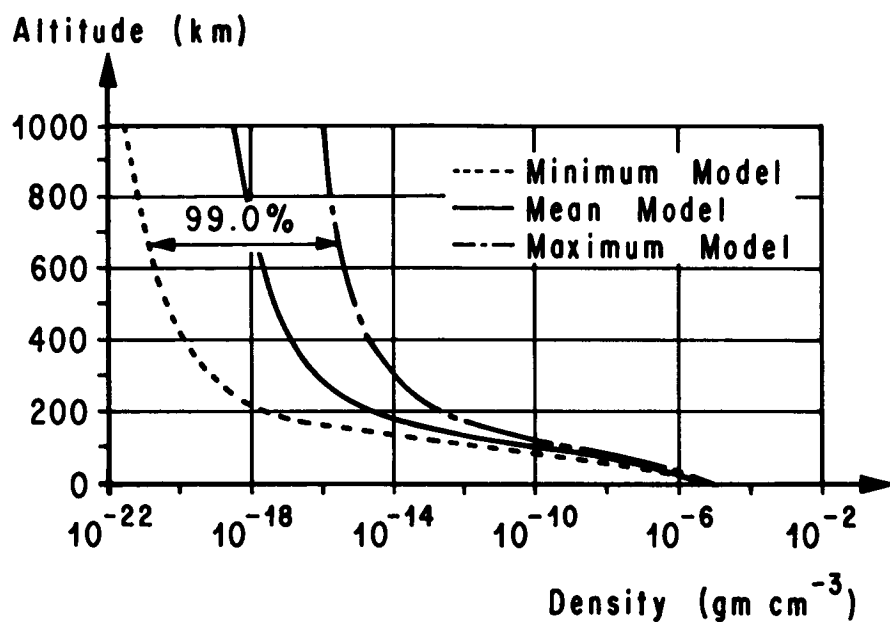


FIG. 3-13. ATMOSPHERIC DENSITY

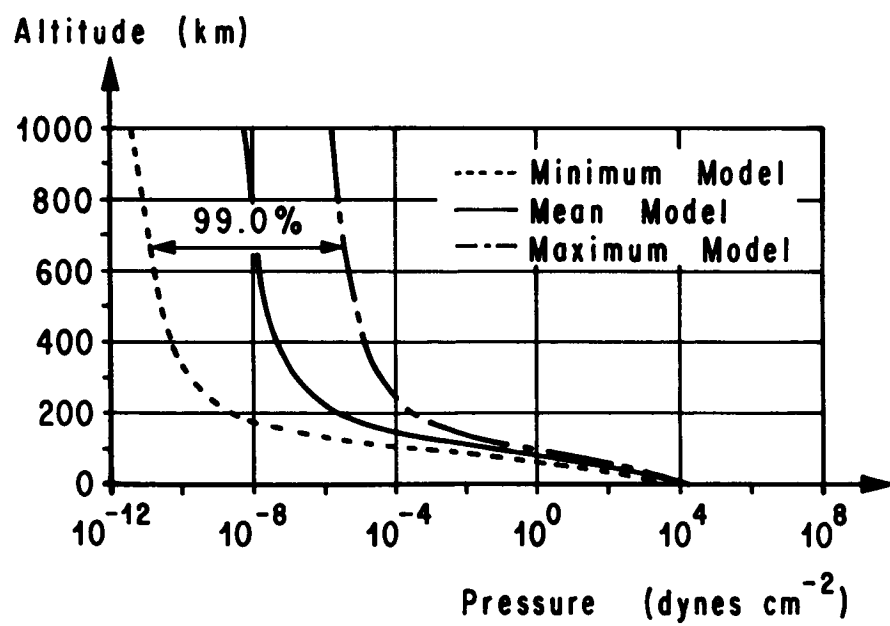


FIG. 3-14. ATMOSPHERIC PRESSURE

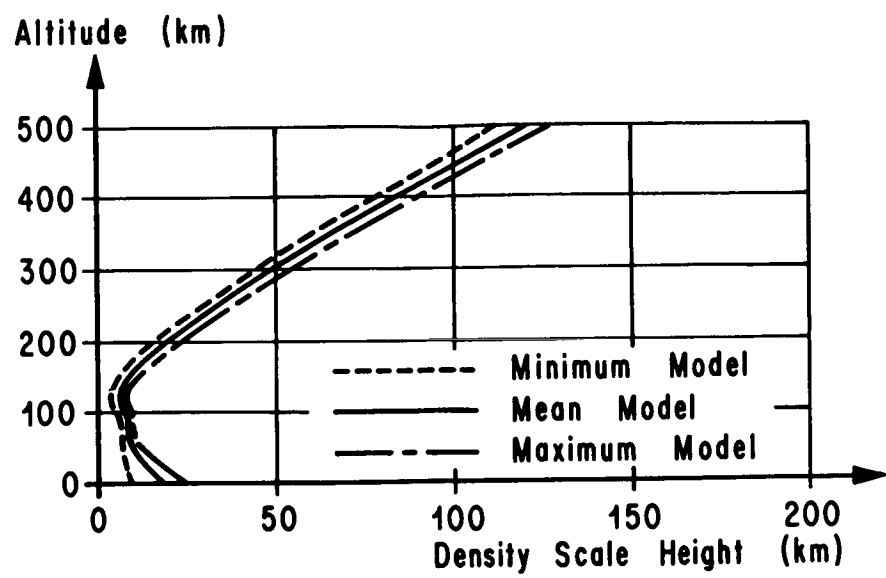


FIG. 3-15. DENSITY SCALE HEIGHT

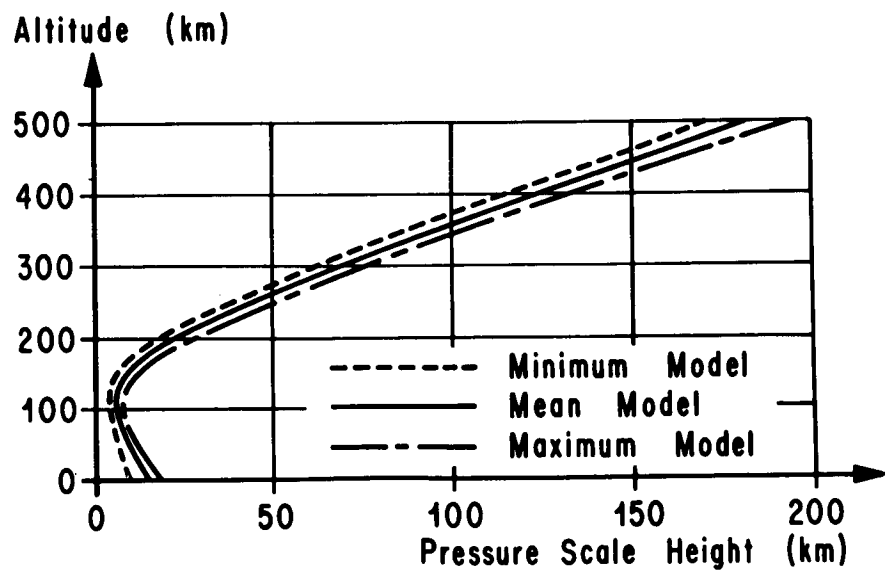


FIG. 3-16. PRESSURE SCALE HEIGHT

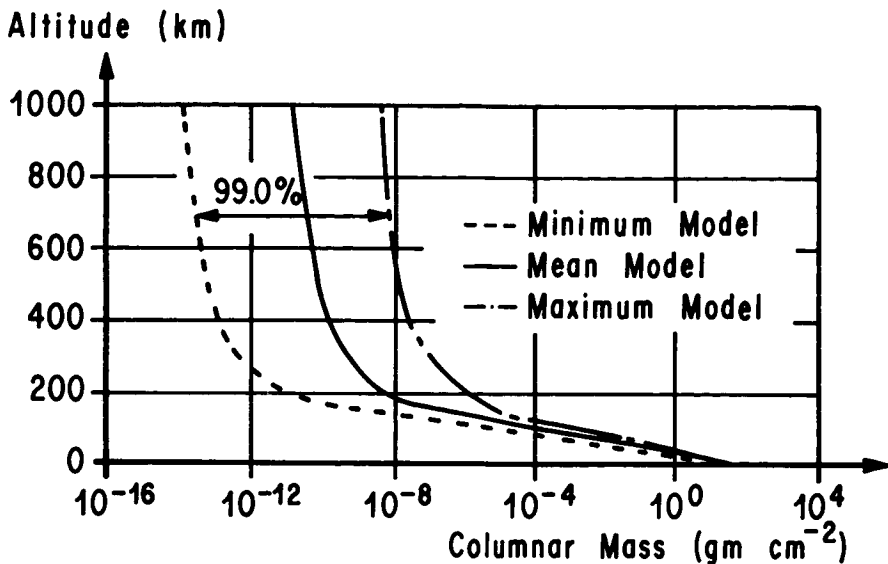


FIG. 3-17. COLUMNAR MASS

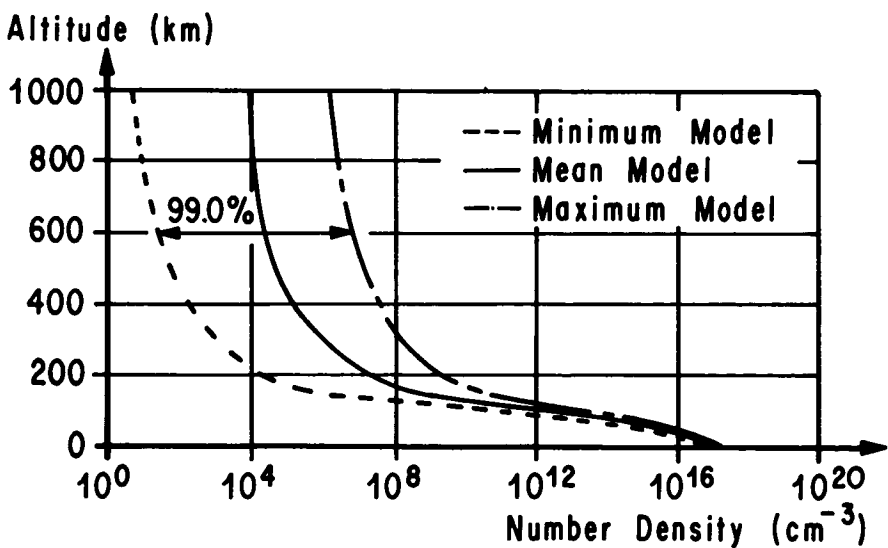


FIG. 3-18. NUMBER DENSITY

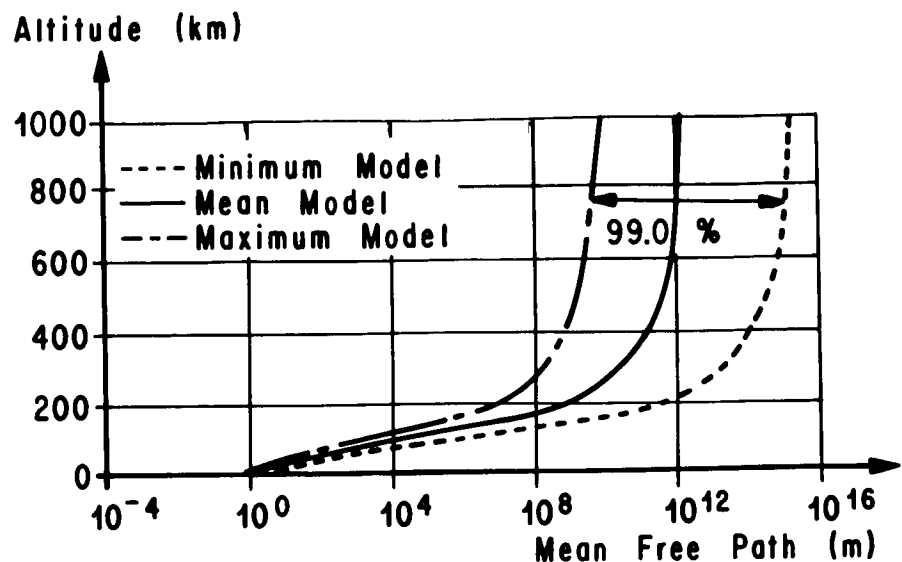


FIG. 3-19. ATMOSPHERIC MEAN FREE PATH

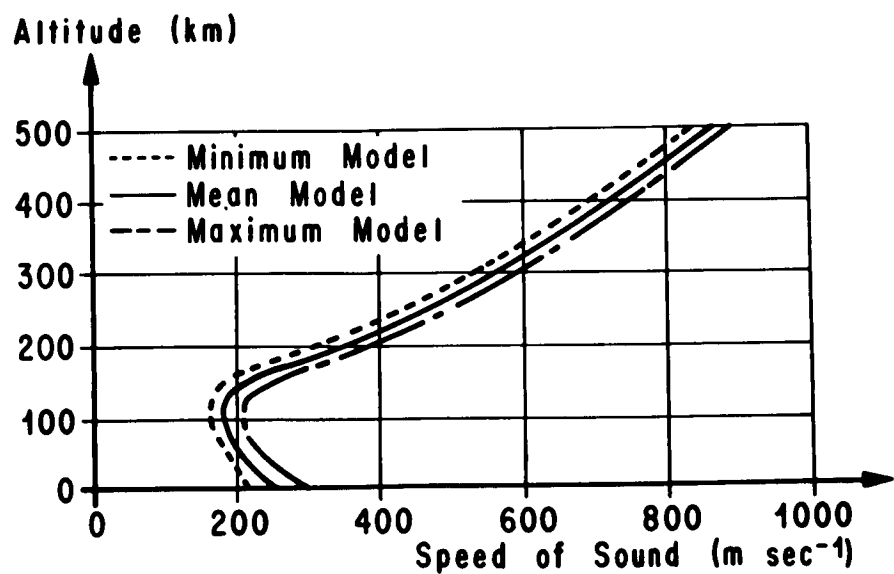


FIG. 3-20. SPEED OF SOUND

TABLE 3.2
**A MEAN MODEL AND 99% CONFIDENCE
 ENVELOPE FOR THE MARS ATMOSPHERE**

KINETIC TEMPERATURE (°K)

GEOMETRIC ALTITUDE (km)	MEAN MODEL	99% CONFIDENCE ENVELOPE	
		MINIMUM MODEL	MAXIMUM MODEL
0.00	2.3000000e+02	1.7500000e+02	2.7500000e+02
1.00	2.2550133e+02	1.7415025e+02	2.7090121e+02
2.00	2.2100532e+02	1.7330101e+02	2.6680485e+02
3.00	2.1651197e+02	1.7245226e+02	2.6271091e+02
4.00	2.1202128e+02	1.7160402e+02	2.5861939e+02
5.00	2.0753323e+02	1.7075628e+02	2.5453028e+02
6.00	2.0304784e+02	1.6990904e+02	2.5044359e+02
7.00	1.9856510e+02	1.6906230e+02	2.4635931e+02
8.00	1.9408501e+02	1.6821606e+02	2.4227745e+02
9.00	1.8960755e+02	1.6737032e+02	2.3819799e+02
10.00	1.8513274e+02	1.6652507e+02	2.3412094e+02
20.00	1.7610588e+02	1.5810000e+02	1.9348234e+02
30.00	1.6723752e+02	1.4972432e+02	1.8423752e+02
40.00	1.5842100e+02	1.4139761e+02	1.7542100e+02
50.00	1.4965569e+02	1.3311926e+02	1.6665569e+02
60.00	1.4094160e+02	1.2488929e+02	1.5794160e+02
70.00	1.3227796e+02	1.1670696e+02	1.4927796e+02
80.00	1.2366421e+02	1.0857176e+02	1.4066421e+02
90.00	1.1510032e+02	1.0048364e+02	1.3210032e+02
100.00	1.0658542e+02	9.2441790e+01	1.2358542e+02
110.00	1.0400000e+02	9.0000000e+01	1.2100000e+02
120.00	1.0400000e+02	9.0000000e+01	1.2100000e+02
130.00	1.0400000e+02	9.0000000e+01	1.2100000e+02
140.00	1.0400000e+02	9.0000000e+01	1.2100000e+02
150.00	1.0400000e+02	9.0000000e+01	1.3437102e+02
160.00	1.1519221e+02	9.0000000e+01	1.6806786e+02
170.00	1.5192010e+02	1.0054799e+02	2.0157491e+02
180.00	1.8844167e+02	1.5177463e+02	2.3489375e+02
190.00	2.2162857e+02	1.9162857e+02	2.6369412e+02
200.00	2.5202163e+02	2.2202163e+02	2.8872370e+02
300.00	4.5354508e+02	4.2854508e+02	4.7854508e+02
400.00	5.8998801e+02	5.6498801e+02	6.1498801e+02
500.00	6.8414188e+02	6.5914188e+02	7.0914188e+02
600.00	7.5765630e+02	7.3361334e+02	7.8169926e+02
700.00	8.1095196e+02	7.9095196e+02	8.3095196e+02
800.00	8.5315593e+02	8.3315593e+02	8.7315593e+02
900.00	8.8539590e+02	8.6431672e+02	9.1039590e+02
1000.00	9.1369662e+02	8.8652246e+02	9.3869562e+02

TABLE 3.2
A MEAN MODEL AND 99% CONFIDENCE
ENVELOPE FOR THE MARS ATMOSPHERE

KINETIC TEMPERATURE (°K)

CONTINUED

GEOMETRIC ALTITUDE (km)	MEAN MODEL	99% CONFIDENCE ENVELOPE	
		MINIMUM MODEL	MAXIMUM MODEL
5000.00	9.13×10^2	8.86×10^2	9.38×10^2
10,000.00	1.30×10^5	1.90×10^5	1.00×10^5
15,000.00	1.90×10^5	1.90×10^5	1.90×10^5
20,000.00	1.90×10^5	1.90×10^5	1.90×10^5
30,000.00	1.90×10^5	1.90×10^5	1.90×10^5

TABLE 3.2
A MEAN MODEL AND 99% CONFIDENCE
ENVELOPE FOR THE MARS ATMOSPHERE

MOLECULAR TEMPERATURE (°K)

GEOMETRIC ALTITUDE (km)	MEAN MODEL	99% CONFIDENCE ENVELOPE	
		MINIMUM MODEL	MAXIMUM MODEL
0.00	2.3000000e+02	1.7500000e+02	2.7500000e+02
1.00	2.2550133e+02	1.7415025e+02	2.7090121e+02
2.00	2.2100532e+02	1.7330101e+02	2.6680485e+02
3.00	2.1651197e+02	1.7245226e+02	2.6271091e+02
4.00	2.1202128e+02	1.7160402e+02	2.5861939e+02
5.00	2.0753323e+02	1.7075628e+02	2.5453028e+02
6.00	2.0304784e+02	1.6990904e+02	2.5044359e+02
7.00	1.9856510e+02	1.6906230e+02	2.4635931e+02
8.00	1.9408501e+02	1.6821606e+02	2.4227745e+02
9.00	1.8960755e+02	1.6737032e+02	2.3819799e+02
10.00	1.8513274e+02	1.6652507e+02	2.3412094e+02
20.00	1.7610588e+02	1.5810000e+02	1.9348234e+02
30.00	1.6723752e+02	1.4972432e+02	1.8423752e+02
40.00	1.5842100e+02	1.4139761e+02	1.7542100e+02
50.00	1.4965569e+02	1.3311926e+02	1.6665569e+02
60.00	1.4125577e+02	1.2565149e+02	1.5794160e+02
70.00	1.3375055e+02	1.1866301e+02	1.4963366e+02
80.00	1.2731122e+02	1.1225837e+02	1.4137737e+02
90.00	1.2134179e+02	1.0616829e+02	1.3369420e+02
100.00	1.1545167e+02	1.0028236e+02	1.2736403e+02
110.00	1.1676896e+02	9.0184190e+01	1.2919937e+02
120.00	1.2121760e+02	9.0661503e+01	1.3440982e+02
130.00	1.2564093e+02	9.1136100e+01	1.3959063e+02
140.00	1.3003914e+02	9.1608002e+01	1.4474201e+02
150.00	1.3441226e+02	9.2077211e+01	1.6992530e+02
160.00	1.5785082e+02	9.2647310e+01	2.2557579e+02
170.00	2.2080475e+02	9.4897975e+01	2.8091284e+02
180.00	2.8340505e+02	9.3568786e+01	3.3593905e+02
190.00	3.4860722e+02	9.31330086e+01	3.9215667e+02
200.00	4.1590565e+02	9.38330569e+01	4.4930999e+02
300.00	1.0765009e+03	9.10764004e+01	1.0674831e+03
400.00	1.8151632e+03	9.18440881e+01	1.7471662e+03
500.00	2.5518395e+03	9.26254365e+01	2.4408763e+03
600.00	3.2921999e+03	9.34409420e+01	3.0992876e+03
700.00	4.0248160e+03	9.42996037e+01	3.7072721e+03
800.00	4.7180834e+03	9.50682474e+01	4.3216589e+03
900.00	5.4630709e+03	9.58659016e+01	5.0274536e+03
1000.00	6.1765408e+03	9.65915815e+01	5.6792024e+03

TABLE 3.2
**A MEAN MODEL AND 99% CONFIDENCE
 ENVELOPE FOR THE MARS ATMOSPHERE**

ATMOSPHERIC PRESSURE (dynes cm⁻²)

GEOMETRIC ALTITUDE (km)	MEAN MODEL	99% CONFIDENCE ENVELOPE	
		MINIMUM MODEL	MAXIMUM MODEL
0.00	8.0000000e+03	4.0000000e+03	1.0000000e+04
1.00	7.3908910e+03	3.5703051e+03	9.4257490e+03
2.00	6.8175960e+03	3.1852137e+03	8.8767825e+03
3.00	6.2786478e+03	2.8402580e+03	8.3523310e+03
4.00	5.7726131e+03	2.5314010e+03	7.8516382e+03
5.00	5.2980918e+03	2.2549974e+03	7.3739605e+03
6.00	4.8537167e+03	2.0077564e+03	6.9185674e+03
7.00	4.4381541e+03	1.7867090e+03	6.4847411e+03
8.00	4.0501027e+03	1.5891771e+03	6.0717766e+03
9.00	3.6882940e+03	1.4127469e+03	5.6789816e+03
10.00	3.3514919e+03	1.2552430e+03	5.3056765e+03
20.00	1.2446852e+03	3.7349884e+02	2.5039650e+03
30.00	4.4179575e+02	1.0479892e+02	1.0773315e+03
40.00	1.4918313e+02	2.7552325e+01	4.4695717e+02
50.00	4.7675169e+01	6.7383171e+00	1.7821452e+02
60.00	1.4338255e+01	1.5247270e+00	6.7991478e+01
70.00	4.0516643e+00	3.1892137e-01	2.4735827e+01
80.00	1.0784462e+00	6.1510292e-02	8.5510337e+00
90.00	2.7091034e-01	1.0904824e-02	2.7957314e+00
100.00	6.4072898e-02	1.7678733e-03	8.6618830e-01
110.00	1.4650152e-02	2.7300224e-04	2.6218149e-01
120.00	3.5473299e-03	4.5983450e-05	8.3350855e-02
130.00	9.1088534e-04	8.4530550e-06	2.7848834e-02
140.00	2.4696388e-04	1.6828432e-06	9.7411429e-03
150.00	7.0448009e-05	3.6055563e-07	3.6444945e-03
160.00	2.1646368e-05	8.2995790e-08	1.7185780e-03
170.00	9.0262761e-06	2.0927921e-08	9.6024768e-04
180.00	4.7104517e-06	8.0983646e-09	5.9742729e-04
190.00	2.8112214e-06	4.2290918e-09	4.0051315e-04
200.00	1.8415965e-06	2.5368893e-09	2.8405250e-04
300.00	1.8905104e-07	1.8996541e-10	3.8775181e-05
400.00	6.5910443e-08	6.0175216e-11	1.4770837e-05
500.00	3.4360915e-08	2.9848149e-11	8.0541959e-06
600.00	2.1694931e-08	1.8314801e-11	5.2227215e-06
700.00	1.5319925e-08	1.2751851e-11	3.7377041e-06
800.00	1.1611862e-08	9.5978070e-12	2.8520364e-06
900.00	9.2546602e-09	7.6085042e-12	2.2862766e-06
1000.00	7.6610476e-09	6.2656711e-12	1.9022788e-06

TABLE 3.2
A MEAN MODEL AND 99% CONFIDENCE
ENVELOPE FOR THE MARS ATMOSPHERE

ATMOSPHERIC PRESSURE (dynes cm^{-2})

CONTINUED

GEOMETRIC ALTITUDE (km)	MEAN MODEL	99% CONFIDENCE ENVELOPE	
		MINIMUM MODEL	MAXIMUM MODEL
5000.00	7.70×10^{-9}	6.30×10^{-12}	1.90×10^{-6}
10,000.00	4.00×10^{-11}	10^{-13}	1.00×10^{-9}
15,000.00	10^{-13}	10^{-13}	1.00×10^{-11}
20,000.00	10^{-13}	10^{-13}	10^{-13}
30,000.00	10^{-13}	10^{-13}	10^{-13}

TABLE 3.2
A MEAN MODEL AND 99% CONFIDENCE
ENVELOPE FOR THE MARS ATMOSPHERE

ATMOSPHERIC DENSITY (gm cm^{-3})

GEOMETRIC ALTITUDE (km)	MEAN MODEL	99% CONFIDENCE ENVELOPE	
		MINIMUM MODEL	MAXIMUM MODEL
0.00	1.6733691e-05	1.2096068e-05	1.5657411e-05
1.00	1.5768025e-05	1.0849345e-05	1.4981578e-05
2.00	1.4840828e-05	9.7265716e-06	1.4325655e-05
3.00	1.3951272e-05	8.7158787e-06	1.3689331e-05
4.00	1.3098532e-05	7.8064895e-06	1.3072295e-05
5.00	1.2281783e-05	6.9886236e-06	1.2474237e-05
6.00	1.1500207e-05	6.2534090e-06	1.1894848e-05
7.00	1.0752985e-05	5.5928007e-06	1.1333820e-05
8.00	1.0039305e-05	4.9995066e-06	1.0790844e-05
9.00	9.3583547e-06	4.4669204e-06	1.0265616e-05
10.00	8.7093259e-06	3.9890590e-06	9.7578275e-06
20.00	3.4002845e-06	1.2502005e-06	5.5723652e-06
30.00	1.2709177e-06	3.7041343e-07	2.5178155e-06
40.00	4.5304002e-07	1.0311895e-07	1.0970766e-06
50.00	1.5325992e-07	2.6787539e-08	4.6044268e-07
60.00	4.8833711e-08	6.4216519e-09	1.8535768e-07
70.00	1.4573622e-08	1.4222978e-09	7.1178656e-08
80.00	4.0753170e-09	2.8996884e-10	2.6043021e-08
90.00	1.0741002e-09	5.4355830e-11	9.0040004e-09
100.00	2.6699539e-10	9.3292959e-12	2.9283175e-09
110.00	6.0359318e-11	1.4186066e-12	8.7376426e-10
120.00	1.4078795e-11	2.2824717e-13	2.6701256e-10
130.00	3.4878851e-12	4.0170096e-14	8.5902025e-11
140.00	9.1366910e-13	7.6719978e-15	2.8977969e-11
150.00	2.5215027e-13	1.5798938e-15	9.2348936e-12
160.00	6.5973235e-14	3.4728034e-16	3.2804197e-12
170.00	1.9666623e-14	7.4339754e-17	1.4718529e-12
180.00	7.9962170e-15	1.8183706e-17	7.6573271e-13
190.00	3.8796119e-15	7.1434467e-18	4.3975401e-13
200.00	2.1302435e-15	3.5025031e-18	2.7221069e-13
300.00	8.4487854e-17	9.3394860e-20	1.5640313e-14
400.00	1.7469005e-17	1.7268646e-20	3.6401856e-15
500.00	6.4780004e-18	6.0164203e-21	1.4207873e-15
600.00	3.1703096e-18	2.8167424e-21	7.2558387e-16
700.00	1.8312187e-18	1.5695209e-21	4.3411330e-16
800.00	1.1840386e-18	1.0021587e-21	2.8415625e-16
900.00	8.1499180e-19	6.8641505e-22	1.9580931e-16
1000.00	5.9672255e-19	5.0303738e-22	1.4422464e-16

TABLE 3.2
A MEAN MODEL AND 99% CONFIDENCE
ENVELOPE FOR THE MARS ATMOSPHERE

ATMOSPHERIC DENSITY (gm cm^{-3})

CONTINUED

GEOMETRIC ALTITUDE (km)	MEAN MODEL	99% CONFIDENCE ENVELOPE	
		MINIMUM MODEL	MAXIMUM MODEL
5000.00	6.0×10^{-19}	5.0×10^{-22}	1.40×10^{-16}
10,000.00	5.0×10^{-21}	10^{-23}	1.00×10^{-19}
15,000.00	10^{-23}	10^{-23}	10^{-23}
20,000.00	10^{-23}	10^{-23}	10^{-23}
30,000.00	10^{-23}	10^{-23}	10^{-23}

TABLE 3.2
**A MEAN MODEL AND 99% CONFIDENCE
 ENVELOPE FOR THE MARS ATMOSPHERE**

MOLECULAR WEIGHT

GEOMETRIC ALTITUDE (km)	MEAN MODEL	99% CONFIDENCE ENVELOPE	
		MINIMUM MODEL	MAXIMUM MODEL
0.00	4.0000000e+01	4.4000000e+01	3.5800000e+01
1.00	4.0000000e+01	4.4000000e+01	3.5800000e+01
2.00	4.0000000e+01	4.4000000e+01	3.5800000e+01
3.00	4.0000000e+01	4.4000000e+01	3.5800000e+01
4.00	4.0000000e+01	4.4000000e+01	3.5800000e+01
5.00	4.0000000e+01	4.4000000e+01	3.5800000e+01
6.00	4.0000000e+01	4.4000000e+01	3.5800000e+01
7.00	4.0000000e+01	4.4000000e+01	3.5800000e+01
8.00	4.0000000e+01	4.4000000e+01	3.5800000e+01
9.00	4.0000000e+01	4.4000000e+01	3.5800000e+01
10.00	4.0000000e+01	4.4000000e+01	3.5800000e+01
20.00	4.0000000e+01	4.4000000e+01	3.5800000e+01
30.00	4.0000000e+01	4.4000000e+01	3.5800000e+01
40.00	4.0000000e+01	4.4000000e+01	3.5800000e+01
50.00	4.0000000e+01	4.4000000e+01	3.5800000e+01
60.00	3.9910462e+01	4.3731387e+01	3.5800000e+01
70.00	3.9556798e+01	4.3270998e+01	3.5714200e+01
80.00	3.8847930e+01	4.2547930e+01	3.5618491e+01
90.00	3.7933369e+01	4.1633369e+01	3.5370011e+01
100.00	3.6915996e+01	4.0544723e+01	3.4729816e+01
110.00	3.5757857e+01	3.9096502e+01	3.3650597e+01
120.00	3.4552360e+01	3.7516886e+01	3.2434708e+01
130.00	3.3353724e+01	3.5946259e+01	3.1225739e+01
140.00	3.2161893e+01	3.4384549e+01	3.0023633e+01
150.00	3.0976862e+01	3.2831750e+01	2.8833569e+01
160.00	2.9589988e+01	3.1356744e+01	2.7658098e+01
170.00	2.8244511e+01	2.9926993e+01	2.6489247e+01
180.00	2.6906592e+01	2.8601127e+01	2.5326962e+01
190.00	2.5693546e+01	2.7276168e+01	2.4252235e+01
200.00	2.4585093e+01	2.5953176e+01	2.3251052e+01
300.00	1.7164797e+01	1.7862597e+01	1.6318098e+01
400.00	1.3054141e+01	1.3538775e+01	1.2654141e+01
500.00	1.0774828e+01	1.1103661e+01	1.0445995e+01
600.00	9.2277333e+00	9.4085925e+00	9.0468740e+00
700.00	8.0809609e+00	8.1210981e+00	8.0408236e+00
800.00	7.2368814e+00	7.2368814e+00	7.2368814e+00
900.00	6.4920819e+00	6.4920819e+00	6.4920819e+00
1000.00	5.9260677e+00	5.9260677e+00	5.9260677e+00

TABLE 3.2
**A MEAN MODEL AND 99% CONFIDENCE
ENVELOPE FOR THE MARS ATMOSPHERE**

DENSITY SCALE HEIGHT (km)

GEOMETRIC ALTITUDE (km)	MEAN MODEL	99% CONFIDENCE ENVELOPE	
		MINIMUM MODEL	MAXIMUM MODEL
0.00	1.6983768e+01	9.2127745e+00	2.2825522e+01
1.00	1.6663064e+01	9.1735854e+00	2.2500882e+01
2.00	1.6340497e+01	9.1342495e+00	2.2173746e+01
3.00	1.6017736e+01	9.0948888e+00	2.1846413e+01
4.00	1.5694781e+01	9.0555032e+00	2.1518883e+01
5.00	1.5371633e+01	9.0160927e+00	2.1191156e+01
6.00	1.5048292e+01	8.9766574e+00	2.0863231e+01
7.00	1.4724757e+01	8.9371973e+00	2.0535109e+01
8.00	1.4401028e+01	8.8977123e+00	2.0206790e+01
9.00	1.4077106e+01	8.8582025e+00	1.9878274e+01
10.00	1.2182156e+01	8.8186678e+00	1.9549561e+01
20.00	1.0395857e+01	8.4219542e+00	1.4549747e+01
30.00	9.9304819e+00	8.0227554e+00	1.2299151e+01
40.00	9.4621996e+00	7.6210709e+00	1.1779351e+01
50.00	8.9909916e+00	7.2168866e+00	1.1256280e+01
60.00	8.5184475e+00	6.8212298e+00	1.0729989e+01
70.00	8.0678695e+00	6.4645606e+00	1.0197027e+01
80.00	7.6736920e+00	6.1315402e+00	9.6933541e+00
90.00	7.3411913e+00	5.8248893e+00	9.1779383e+00
100.00	7.0262843e+00	5.5287197e+00	8.6998958e+00
110.00	6.7231745e+00	5.3340281e+00	8.2462147e+00
120.00	7.0193575e+00	5.6160625e+00	8.6279973e+00
130.00	7.3171242e+00	5.8996224e+00	9.0118284e+00
140.00	7.6164403e+00	6.1846805e+00	9.3976533e+00
150.00	7.9173830e+00	6.4712959e+00	8.3359030e+00
160.00	6.9352856e+00	6.7708941e+00	1.1128704e+01
170.00	9.7561000e+00	5.5827997e+00	1.3937151e+01
180.00	1.2592690e+01	8.8818864e+00	1.6761235e+01
190.00	1.5209209e+01	1.2628303e+01	1.9408524e+01
200.00	1.8247090e+01	1.5536645e+01	2.2361840e+01
300.00	4.8243969e+01	4.4631056e+01	5.2548037e+01
400.00	8.3286635e+01	7.8060110e+01	8.7332386e+01
500.00	1.2101119e+02	1.1428555e+02	1.2818206e+02
600.00	1.5978616e+02	1.4825150e+02	1.7273712e+02
700.00	2.0719133e+02	1.9653736e+02	2.1894761e+02
800.00	2.5383514e+02	2.4938512e+02	2.5823197e+02
900.00	2.9135965e+02	2.9272241e+02	2.9712857e+02
1000.00	3.5543530e+02	3.5621212e+02	3.6229993e+02

TABLE 3.2
**A MEAN MODEL AND 99% CONFIDENCE
 ENVELOPE FOR THE MARS ATMOSPHERE**

PRESSURE SCALE HEIGHT (km)

GEOMETRIC ALTITUDE (km)	MEAN MODEL	99% CONFIDENCE ENVELOPE	
		MINIMUM MODEL	MAXIMUM MODEL
0.00	1.2748731e+01	8.8182924e+00	1.7031339e+01
1.00	1.2506768e+01	8.7806651e+00	1.6787418e+01
2.00	1.2264660e+01	8.7430141e+00	1.6543350e+01
3.00	1.2022407e+01	8.7053393e+00	1.6299135e+01
4.00	1.1780008e+01	8.6676408e+00	1.6054773e+01
5.00	1.1537464e+01	8.6299184e+00	1.5810264e+01
6.00	1.1294774e+01	8.5921723e+00	1.5565607e+01
7.00	1.1051940e+01	8.5544023e+00	1.5320804e+01
8.00	1.0808960e+01	8.5166086e+00	1.5075853e+01
9.00	1.0565835e+01	8.4787911e+00	1.4830755e+01
10.00	1.0322564e+01	8.4409498e+00	1.4585509e+01
20.00	9.8772468e+00	8.0612284e+00	1.2124961e+01
30.00	9.4350877e+00	7.6791279e+00	1.1613611e+01
40.00	8.9901653e+00	7.2946476e+00	1.1122783e+01
50.00	8.5424700e+00	6.9077792e+00	1.0628876e+01
60.00	8.1100647e+00	6.5583271e+00	1.0131917e+01
70.00	7.7238579e+00	6.2296175e+00	9.6548373e+00
80.00	7.3946680e+00	5.9275884e+00	9.1750587e+00
90.00	7.0887295e+00	5.6384555e+00	8.7266499e+00
100.00	6.7835501e+00	5.3565938e+00	8.3614306e+00
110.00	6.9004260e+00	5.4711964e+00	8.5307231e+00
120.00	7.2044147e+00	5.7604812e+00	8.9256733e+00
130.00	7.5100286e+00	6.0513305e+00	9.3227420e+00
140.00	7.8172669e+00	6.3437436e+00	9.7219284e+00
150.00	8.1261178e+00	6.6377089e+00	1.1478344e+01
160.00	9.5972652e+00	6.9904657e+00	1.5323927e+01
170.00	1.3500770e+01	8.2810365e+00	1.9191048e+01
180.00	1.7426105e+01	1.3174595e+01	2.3079702e+01
190.00	2.1555836e+01	1.7611542e+01	2.7093497e+01
200.00	2.5861413e+01	2.1667560e+01	3.1216231e+01
300.00	7.0728561e+01	6.4292689e+01	7.8364326e+01
400.00	1.2582815e+02	1.1621204e+02	1.3532353e+02
500.00	1.8637576e+02	1.7431907e+02	1.9918600e+02
600.00	2.5299931e+02	2.4039078e+02	2.6611662e+02
700.00	3.2503341e+02	3.1565867e+02	3.3451331e+02
800.00	3.9992148e+02	3.9054784e+02	4.0929512e+02
900.00	4.8548530e+02	4.7389413e+02	4.9918817e+02
1000.00	5.7483157e+02	5.5768920e+02	5.9055399e+02

TABLE 3.2
**A MEAN MODEL AND 99% CONFIDENCE
 ENVELOPE FOR THE MARS ATMOSPHERE**

NUMBER DENSITY (cm^{-3})

GEOMETRIC ALTITUDE (km)	MEAN MODEL	99% CONFIDENCE ENVELOPE	
		MINIMUM MODEL	MAXIMUM MODEL
0.00	2.5200041e+17	1.6560027e+17	2.6345498e+17
1.00	2.3745799e+17	1.4853210e+17	2.5208327e+17
2.00	2.2349491e+17	1.3316086e+17	2.4104657e+17
3.00	2.1009867e+17	1.1932405e+17	2.3033965e+17
4.00	1.9725686e+17	1.0687413e+17	2.1995726e+17
5.00	1.8495706e+17	9.5677202e+16	2.0989421e+17
6.00	1.7318694e+17	8.5611804e+16	2.0014528e+17
7.00	1.6193419e+17	7.6567797e+16	1.9070530e+17
8.00	1.5118655e+17	6.8445352e+16	1.8156908e+17
9.00	1.4093180e+17	6.1154022e+16	1.7273147e+17
10.00	1.3115777e+17	5.4611899e+16	1.6418731e+17
20.00	5.1206461e+16	1.7115772e+16	9.3761821e+16
30.00	1.9139338e+16	5.0711159e+15	4.2365308e+16
40.00	6.8225396e+15	1.4117418e+15	1.8459649e+16
50.00	2.3080122e+15	3.6673270e+14	7.7475080e+15
60.00	7.3540949e+14	8.7915120e+13	3.1188684e+15
70.00	2.1947092e+14	1.9471856e+13	1.1976674e+15
80.00	6.1372087e+13	3.9697956e+12	4.3820550e+14
90.00	1.6175373e+13	7.4415421e+11	1.5150326e+14
100.00	4.0208074e+12	1.2772199e+11	4.9272503e+13
110.00	9.0897894e+11	1.9421323e+10	1.4702146e+13
120.00	2.1201910e+11	3.1247999e+09	4.4928110e+12
130.00	5.2525678e+10	5.4994554e+08	1.4454060e+12
140.00	1.3759366e+10	1.0503288e+08	4.8758956e+11
150.00	3.7972478e+09	2.1629412e+07	1.5538832e+11
160.00	9.9352153e+08	4.7544142e+06	5.5197051e+10
170.00	2.9616879e+08	1.0177425e+06	2.4765715e+10
180.00	1.2041874e+08	2.4894259e+05	1.2884384e+10
190.00	5.8424874e+07	9.7796795e+04	7.3993960e+09
200.00	3.2080325e+07	4.7950743e+04	4.5802759e+09
300.00	1.2723417e+06	1.2786150e+03	2.6316729e+08
400.00	2.6307384e+05	2.3641504e+02	6.1250550e+07
500.00	9.7555210e+04	8.2367329e+01	2.3906473e+07
600.00	4.7743162e+04	3.8562391e+01	1.2208831e+07
700.00	2.7577171e+04	2.1487402e+01	7.3044842e+06
800.00	1.7830985e+04	1.3719975e+01	4.7812745e+06
900.00	1.2273339e+04	9.3973113e+00	3.2947298e+06
1000.00	8.9863215e+03	6.8867937e+00	2.4267549e+06

TABLE 3.2
**A MEAN MODEL AND 99% CONFIDENCE
 ENVELOPE FOR THE MARS ATMOSPHERE**

SPEED OF SOUND (m sec^{-1})

GEOMETRIC ALTITUDE (km)	MEAN MODEL	99% CONFIDENCE ENVELOPE	
		MINIMUM MODEL	MAXIMUM MODEL
0.00	2.5870995e+02	2.1516513e+02	2.9902262e+02
1.00	2.5616735e+02	2.1464211e+02	2.9678584e+02
2.00	2.5360078e+02	2.1411812e+02	2.9453341e+02
3.00	2.5100951e+02	2.1359315e+02	2.9226496e+02
4.00	2.4839276e+02	2.1306720e+02	2.8998013e+02
5.00	2.4574973e+02	2.1254026e+02	2.8767851e+02
6.00	2.4307954e+02	2.1201233e+02	2.8535971e+02
7.00	2.4038130e+02	2.1148339e+02	2.8302330e+02
8.00	2.3765404e+02	2.1095343e+02	2.8066884e+02
9.00	2.3489676e+02	2.1042246e+02	2.7829586e+02
10.00	2.3210839e+02	2.0989046e+02	2.7590389e+02
20.00	2.2637900e+02	2.0451200e+02	2.5081780e+02
30.00	2.2060537e+02	1.9902107e+02	2.4475228e+02
40.00	2.1471164e+02	1.9340776e+02	2.3882428e+02
50.00	2.0868721e+02	1.8766070e+02	2.3278113e+02
60.00	2.0274601e+02	1.8232100e+02	2.2661360e+02
70.00	1.9728633e+02	1.7717831e+02	2.2057300e+02
80.00	1.9247865e+02	1.7233054e+02	2.1440142e+02
90.00	1.8791196e+02	1.6759084e+02	2.0849420e+02
100.00	1.8329445e+02	1.6287902e+02	2.0349844e+02
110.00	1.8433717e+02	1.6414064e+02	2.0495943e+02
120.00	1.8781577e+02	1.6794307e+02	2.0905146e+02
130.00	1.9121184e+02	1.7164037e+02	2.1304229e+02
140.00	1.9452986e+02	1.7523934e+02	2.1693769e+02
150.00	1.9777376e+02	1.7874595e+02	2.3505350e+02
160.00	2.1432491e+02	1.8291611e+02	2.7082200e+02
170.00	2.5348568e+02	1.9852559e+02	3.0222021e+02
180.00	2.8717922e+02	2.4970169e+02	3.3049732e+02
190.00	3.1850584e+02	2.8789470e+02	3.5708163e+02
200.00	3.4789375e+02	3.1843846e+02	3.8221765e+02
300.00	5.5970143e+02	5.3362946e+02	5.8913959e+02
400.00	7.2678683e+02	6.9846348e+02	7.5371091e+02
500.00	8.6173929e+02	8.3340026e+02	8.9086231e+02
600.00	9.7879629e+02	9.5409485e+02	1.0038496e+03
700.00	1.0822366e+03	1.0665153e+03	1.0979054e+03
800.00	1.1717421e+03	1.1579286e+03	1.1853946e+03
900.00	1.2608622e+03	1.2457195e+03	1.2785324e+03
1000.00	1.3406699e+03	1.3205282e+03	1.3588808e+03

TABLE 3.2
**A MEAN MODEL AND 99% CONFIDENCE
 ENVELOPE FOR THE MARS ATMOSPHERE**

COLUMNAR MASS (gm cm⁻²)

GEOMETRIC ALTITUDE (km)	MEAN MODEL	99% CONFIDENCE ENVELOPE	
		MINIMUM MODEL	MAXIMUM MODEL
0.00	2.1333333e+01	1.0666667e+01	2.6666667e+01
1.00	1.9720703e+01	9.5264463e+00	2.5150202e+01
2.00	1.8201771e+01	8.5039553e+00	2.3699434e+01
3.00	1.6772787e+01	7.5874682e+00	2.2312426e+01
4.00	1.5430080e+01	6.7663847e+00	2.0987273e+01
5.00	1.4170063e+01	6.0311252e+00	1.9722098e+01
6.00	1.2989224e+01	5.3730368e+00	1.8515053e+01
7.00	1.1884135e+01	4.7843067e+00	1.7364322e+01
8.00	1.0851445e+01	4.2578841e+00	1.6268118e+01
9.00	9.8878831e+00	3.7874085e+00	1.5224683e+01
10.00	8.9902578e+00	3.3671447e+00	1.4232288e+01
20.00	3.3585450e+00	1.0078152e+00	6.7564710e+00
30.00	1.1991220e+00	2.8444521e-01	2.9240929e+00
40.00	4.0729047e-01	7.5221638e-02	1.2202546e+00
50.00	1.3092183e-01	1.8504241e-02	4.8939881e-01
60.00	3.9604456e-02	4.2115294e-03	1.8780287e-01
70.00	1.1256458e-02	8.8603714e-04	6.8721834e-02
80.00	3.0135616e-03	1.7188159e-04	2.3894624e-02
90.00	7.6140058e-04	3.0648293e-05	7.8574759e-03
100.00	1.8111766e-04	4.9973249e-06	2.4484924e-03
110.00	4.1650501e-05	7.7614756e-07	7.4538410e-04
120.00	1.0142948e-05	1.3148135e-07	2.3832668e-04
130.00	2.6194117e-06	2.4308253e-08	8.0084242e-05
140.00	7.1423952e-07	4.8669187e-09	2.8172173e-05
150.00	2.0490028e-07	1.0486875e-09	1.0600128e-05
160.00	6.3316264e-08	2.4276513e-10	5.0268914e-06
170.00	2.6551457e-08	6.1561021e-11	2.8246399e-06
180.00	1.3934292e-08	2.3956296e-11	1.7672883e-06
190.00	8.3628276e-09	1.2580711e-11	1.1914474e-06
200.00	5.5091107e-09	7.5890698e-12	8.4973918e-07
300.00	5.9757043e-10	6.0046067e-13	1.2256426e-07
400.00	2.1980925e-10	2.0068246e-13	4.9260276e-08
500.00	1.2073423e-10	1.0487768e-13	2.8300093e-08
600.00	8.0208616e-11	6.7711892e-14	1.9308992e-08
700.00	5.9520727e-11	4.9543287e-14	1.4521668e-08
800.00	4.7352246e-11	3.9139091e-14	1.1630377e-08
900.00	3.9566654e-11	3.2528806e-14	9.7745691e-09
1000.00	3.4301496e-11	2.8053851e-14	8.5172436e-09

TABLE 3.2
A MEAN MODEL AND 99% CONFIDENCE
ENVELOPE FOR THE MARS ATMOSPHERE

MEAN FREE PATH (m)

GEOMETRIC ALTITUDE (km)	MEAN MODEL	99% CONFIDENCE ENVELOPE	
		MINIMUM MODEL	MAXIMUM MODEL
0.00	6.7055769e-06	1.0204139e-05	6.4140301e-06
1.00	7.1162404e-06	1.1376720e-05	6.7033729e-06
2.00	7.5608352e-06	1.2689976e-05	7.0102973e-06
3.00	8.0429263e-06	1.4161505e-05	7.3361585e-06
4.00	8.5665369e-06	1.5811199e-05	7.6824386e-06
5.00	9.1362185e-06	1.7661555e-05	8.0507613e-06
6.00	9.7571337e-06	1.9738028e-05	8.4429078e-06
7.00	1.0435154e-05	2.2069437e-05	8.8608349e-06
8.00	1.1176974e-05	2.4688428e-05	9.3066955e-06
9.00	1.1990254e-05	2.7632003e-05	9.7828621e-06
10.00	1.2883782e-05	3.0942124e-05	1.0291953e-05
20.00	3.2999901e-05	9.8728129e-05	1.8022348e-05
30.00	8.8289790e-05	3.3322215e-04	3.9886601e-05
40.00	2.4768023e-04	1.1969668e-03	9.1540645e-05
50.00	7.3214870e-04	4.6077379e-03	2.1810989e-04
60.00	2.2926351e-03	1.9103564e-02	5.4180168e-04
70.00	7.6141521e-03	8.5344252e-02	1.4075345e-03
80.00	2.6740800e-02	4.1161862e-01	3.8366490e-03
90.00	9.9070540e-02	2.1486384e+00	1.1019645e-02
100.00	3.8786334e-01	1.2191394e+01	3.3269956e-02
110.00	1.6618624e+00	7.7311451e+01	1.0803548e-01
120.00	6.8846227e+00	4.6109381e+02	3.4075813e-01
130.00	2.6825639e+01	2.5102602e+03	1.0197113e+00
140.00	9.8746241e+01	1.2572533e+04	2.9064524e+00
150.00	3.4462430e+02	5.8295368e+04	8.7585945e+00
160.00	1.2581862e+03	2.5329037e+05	2.3651616e+01
170.00	4.0287672e+03	1.1293014e+06	5.0486252e+01
180.00	9.4393488e+03	4.4123370e+06	9.2784154e+01
190.00	1.8578202e+04	1.0711332e+07	1.5470697e+02
200.00	3.2375055e+04	2.0786429e+07	2.3961023e+02
300.00	5.6991792e+05	5.3652447e+08	2.9267928e+03
400.00	2.0962741e+06	2.1993229e+09	9.7516267e+03
500.00	4.6659201e+06	5.1772119e+09	2.0624750e+04
600.00	8.1650954e+06	9.3701261e+09	3.4976700e+04
700.00	1.2379146e+07	1.4514951e+10	5.1959547e+04
800.00	1.7145633e+07	2.0257361e+10	7.1443406e+04
900.00	2.2345942e+07	2.6531702e+10	9.3007626e+04
1000.00	2.7858778e+07	3.3047169e+10	1.1526436e+05

TABLE 3.2
**A MEAN MODEL AND 99% CONFIDENCE
 ENVELOPE FOR THE MARS ATMOSPHERE**

COEFFICIENT
 OF
 VISCOSITY
 (KG/M-SEC)

GEOMETRIC ALTITUDE (km)	MEAN MODEL	99% CONFIDENCE ENVELOPE	
		MINIMUM MODEL	MAXIMUM MODEL
0.00	1.4940314e-05	1.1826620e-05	1.7252215e-05
1.00	1.4698380e-05	1.1775645e-05	1.7049269e-05
2.00	1.4454469e-05	1.1724606e-05	1.6844993e-05
3.00	1.4208544e-05	1.1673503e-05	1.6639365e-05
4.00	1.3960565e-05	1.1622336e-05	1.6432361e-05
5.00	1.3710493e-05	1.1571103e-05	1.6223958e-05
6.00	1.3458288e-05	1.1519805e-05	1.6014132e-05
7.00	1.3203908e-05	1.1468443e-05	1.5802860e-05
8.00	1.2947311e-05	1.1417015e-05	1.5590115e-05
9.00	1.2688456e-05	1.1365521e-05	1.5375873e-05
10.00	1.2427300e-05	1.1313961e-05	1.5160108e-05
20.00	1.1892818e-05	1.0794711e-05	1.2912611e-05
30.00	1.1357427e-05	1.0268691e-05	1.2374754e-05
40.00	1.0814674e-05	9.7357411e-06	1.1851839e-05
50.00	1.0264340e-05	9.1957163e-06	1.1321935e-05
60.00	9.7265745e-06	8.6996590e-06	1.0784855e-05
70.00	9.2372601e-06	8.2276461e-06	1.0262942e-05
80.00	8.8106485e-06	7.7883704e-06	9.7344335e-06
90.00	8.4094725e-06	7.3646971e-06	9.2335545e-06
100.00	8.0081930e-06	6.9497021e-06	8.8141727e-06
110.00	8.0984081e-06	7.0601862e-06	8.9363969e-06
120.00	8.4010680e-06	7.3959739e-06	9.2805817e-06
130.00	8.6989518e-06	7.7263082e-06	9.6187399e-06
140.00	8.9921492e-06	8.0512597e-06	9.9510169e-06
150.00	9.2807418e-06	8.3708985e-06	1.1520791e-05
160.00	1.0779205e-05	8.7546546e-06	1.4702401e-05
170.00	1.4443538e-05	1.0221446e-05	1.7542473e-05
180.00	1.7663942e-05	1.5243229e-05	2.0113302e-05
190.00	2.0674860e-05	1.9082732e-05	2.2530036e-05
200.00	2.3496962e-05	2.2161915e-05	2.4809247e-05
300.00	4.3387503e-05	4.3385101e-05	4.3171471e-05
400.00	5.8556250e-05	5.9074083e-05	5.7321104e-05
500.00	7.0597681e-05	7.1691829e-05	6.8915782e-05
600.00	8.0942373e-05	8.2866893e-05	7.8376810e-05
700.00	9.0028159e-05	9.3209722e-05	8.6206616e-05
800.00	9.7857744e-05	1.0158460e-04	9.3460420e-05
900.00	1.0562994e-04	1.0960419e-04	1.0115746e-04
1000.00	1.1257349e-04	1.1642299e-04	1.0778040e-04

Table 3-3. ESTIMATED NEAR SURFACE WINDS AND VERTICAL WIND SHEARS

Winds		
Near Surface Winds		
Wind Parameters	Surface Pressure	
Continuous Surface Wind	(7 mb)	(14 mb)
Speed (one meter above surface)	50 m/sec	35 m/sec
Peak Surface Wind Speed	43 m/sec	101 m/sec
Vertical Wind Shears*		
$\frac{dv}{dh} = 2 \text{m/sec/km.}$		

*These wind shears are considered to be the average design wind speed gradients for use up to altitudes of 15 km above the surface.

Table 3-4. MARTIAN CLOUDS

	(Dust) YELLOW CLOUDS	BLUE-WHITE CLOUDS	BLUE HAZE OR VIOLET LAYER
Composition	Probably dust; 1956 "storm"; color of dust closely matched planet's desert areas. (some H_2O)?		
Photo Char. In:	(Most can be seen visually)	Blue light shows bright clouds almost always around autumn-winter pole; shows, weaker in yellow light; vanish in red light indicating they consist of fine ice crystals.	Obscures surface in blue, especially $\lambda < 4550\text{\AA}$. Begins abruptly at $\sim 4550\text{\AA}$.
Blue	Not conspicuous in blue		
Red	Bright & impenetrable in red		
Yellow			
Geo. Locales	Great yellow clouds sometimes extend over vast areas of middle latitudes.	Commonly over poles; Various times anywhere on planet; "W" clouds in Tharsis*	Not uniform over entire planet
Diurnal Var.		*"W" clouds are afternoon phenomenon (prominent in blue light, never present in fore noon).	Quick changes in state; random from opacity to near transparency.
Seasonal Var.		At poles: common at Martian equinox; advent during vernal equinox of S. hemisphere; persist April into May; vanish for summer	High level phenomenon. Seems to clear at or near oppositions sometimes for a few days at a time - cannot be predicted on present knowledge.
Height	1956 blue & yellow photos showed dust clouds higher than blue-white polar winter cloud cover.	Meas. of blue photos 1956 for diam. indicate cloud level ht. at poles & equator differs by a const. amt.	Red & Yellow photos seem to be totally unaffected by deg. of opacity of blue haze.
Motions	Various clouds N 6 to 12 mi/hr; southerly 23 mi/hr; av. velocity 20 mph	Immobile compared to yellow clouds.	Some observations have shown tenuous band(veils) patterns indicative of a circulatory system. (1954)

Surface details on Mars, generally, are clearly seen in any light of wavelength greater than 4500 - 4550^oA; i. e., red or yellow light. The so-called "blue haze" is a diffuse, variable phenomenon which occasionally clears and allows surface features to be observed in blue light (blue clearing). The haze itself, which is probably a high-altitude layer, is not blue but causes extinction of solar blue light reflected from the Martian surface while being transparent to longer wavelengths of light. When the effects of observational selection are removed, there is some correlation of blue clearing with favorable oppositions; however, blue clearing also has been observed at unfavorable oppositions, several months from opposition, and on small topographical scales of Mars down to the limit of telescopic resolution.

Some authorities discount the hypothesis that the blue haze is produced by scattering of light by condensed particles, but suggest that the blue haze and its occasional clearing may be accounted for by selective absorption of light by solid particles in the Martian atmosphere.

Others have suggested that solar wind protons interacting

with the CO₂ and N₂ of the Martian atmosphere cause the blue haze by producing molecular ions (CO₂⁺, CO⁺ and N₂⁺) which have strong absorption bands in the required energies. Newer and lower Martian density estimates, particularly those obtained from Mariner IV, would allow a sufficient solar proton flux to account for the phenomena. Also, a reduction in proton flux caused by Mars being in the Earth-induced wake of a solar wind magnetohydrodynamic shock might account for the blue clearings observed on Mars. Some authorities point out that the only acceptable explanation of the blue haze phenomenon is that obscuration is largely due to absorption in blue and violet rather than scattering. A haze of solid CO₂ or ice is unlikely since neither absorbs in the blue or violet region of the spectrum.

3.3 IONOSPHERE

The Martian ionosphere is produced by upper atmospheric ultraviolet photoionization of its constituents. The height and extent of the ionosphere are complex functions of the composition and variation of density with altitude. At the uppermost altitudes, the number density of molecules is too low to produce an appreciable electron density. At lower altitudes, attenuation of the ultraviolet radiation by the atmosphere above, and larger electron recombina-

tion rates due to the increased density of molecules, limit the electron density. These two factors can be expected to cause the Martian ionosphere to occupy a well-defined region. However, the possible atmospheric penetration of the solar wind does not preclude the existence of detectable electron concentrations at the Martian surface.

Measurements of the Martian ionosphere made by the Mariner IV probe have three possible interpretations:

- 1) The ions are mostly O^+ (F2 Model), and the peak electron density of $10^5/cm^3$ occurs at a neutral concentration of $10^9/cm^3$.
- 2) The ions are mostly O_2^+ (E Model) and the peak electron density of $10^5/cm^3$ occurs at a neutral concentration of $5 \times 10^{10}/cm^3$.
- 3) CO_2^+ is the predominant ion (F1 Model).

An estimation of the height of the ionosphere based on this data is strongly dependent on the model of the atmosphere used. The spread in altitudes for a neutral concentration of $10^9/cm^3$ varies from 120 to 190 km for the models of atmospheres used in this report.

3.4 MAGNETIC FIELD

The results of Mariner IV magnetometer measurements to

within about 4 Mars radii show a field strength less than .001 that of the Earth. From this it is inferred that the magnetic moment of Mars is less than 0.001 that of the Earth and that the equatorial surface magnetic field of Mars is less than 200 gammas.

3.5 RADIATION

3.5.1 Solar Thermal Radiation

In the vicinity of Mars beyond the Martian atmosphere, the solar radiation will be assumed to have the same spectrum as that given in Fig. 1-1. The integrated intensity will be varying from 500 to 735 watts/m², depending on the Sun-Mars distance at encounter.

On the Martian surface, the spectral irradiance of solar radiation will not be quite the same as that on the Earth's surface owing to the different compositions of the planetary atmospheres between these two planets. The Martian atmosphere consists primarily of carbon dioxide with possible secondary constituents of argon and nitrogen with traces of water-vapor. The absorption spectrum will then be a band in the far ultraviolet around 900 Å due to N₂ absorption, a band between 1000-2000 Å due to CO₂ absorption, and many bands almost continuous from infrared to the long wavelength end due to CO₂ and water-vapor which is the part not very different from that of the Earth. The significant difference between this

spectrum and that of the Earth's atmosphere is that it does not have the absorption band in the ultraviolet region due to O₃ and O₂.

Therefore, the solar ultraviolet from 2000 to 3000 Å can penetrate the Martian atmosphere and arrive at the Martian surface.

The Martian thermal emission spectrum consists of two parts; the emission from Mars itself and the emission from its atmosphere. The former can be assumed to be a blackbody emission of 280°K with a peak intensity around 10 μ wavelength. The latter does not have enough data for reliable estimation. However, for their combined effect, an assumption could be made as follows:

It varies from \approx 168 watts/m² at 200 km to 3 watts/m² at 2×10^4 km when measured on the Sun-Mars line. The variation in this range of altitude is given in Table 3-9 in Paragraph 3.8.

3.5.2 Magnetically Trapped Radiation

Mariner IV measurements did not detect any trapped radiation belts beyond 4 Martian radii, its limit of detection.

3.5.3 Galactic Cosmic Radiation

- Composition: ~ 85% protons (H⁺)
~ 14% alpha particles (He⁺⁺)
~ 1% nuclei of elements Li → Fe
(in approximate cosmic abundance).

- Flux at sunspot maximum: ~ 4 protons/cm² -sec
(isotropic)
- Integrated yearly rate: ~ 1.3×10^8 protons/cm²
- Flux at sunspot minimum: ~ 2.0 ± 0.3 protons/cm²-sec (isotropic)
- Integrated yearly rate: ~ 7×10^7 protons/cm²
Energy range: 40 MeV to 10^{13} MeV; predomi-
nant energy 10^3 - 10^7 MeV
- Integrated dosage: ~ 6 to 20 rads/yr or
(Independent of shielding) ~ 0.7 to 2.3 millirads/hr

3.5.4

Solar Cosmic Radiation

- Composition: Predominantly of protons (H^+) and alpha (He^{++})
- Integrated yearly flux:
Energy: 30 MeV N ~ 6×10^9 protons/cm² (near
solar maximum)
N ~ 1×10^9 protons/cm² (near
solar minimum)
Energy: 100 MeV N ~ 1×10^9 protons/cm² (near
solar maximum)
N ~ 1×10^8 protons/cm² (near
solar minimum)

- Maximum dosage with shielding of 5 gm/cm² :

~200 rads per flare, skin dose.

The flux and energy of this environmental parameter at the orbit of Mars will probably be reduced; however, this spectrum will be considered as a design criterion.

3.6 METEOROIDS

The meteoroid flux (cometary and asteroidal) of the Martian environment from 10 Mars radii to the Martian sensible atmosphere varies as described in Table 1-5 of Paragraph 1.6.

3.7 GRAVITY

If Mars is considered to be an oblate spheroid, its gravitational potential function can readily be developed in a spherical harmonic series. Truncating after the first two terms, the gravitational potential function can be expressed as

$$\phi(R, \theta) = \frac{GM}{R} \left[1 - J_2 \left(\frac{R_E}{R} \right)^2 P_2^0 \right]$$

and the radial acceleration of gravity as

$$z = -\frac{\partial \phi}{\partial R} = \frac{GM}{R^2} \left[1 - 3J_2 \left(\frac{R_E}{R} \right)^2 P_2^0 \right]$$

in which

$$P_2^o = \frac{3}{2} \sin^2 \theta - \frac{1}{2}$$

θ = latitude

R_E = equatorial radius = 3381 km

GM = $.429778 \times 10^5$ km³/sec²

J_2 = $.1947 \times 10^{-2}$

R = distance from center of Mars (km).

The constant J_2 is a measure of the flattening, $f = (\frac{1}{192})$.

The components of the gravitational vector are obtained from the potential function in the usual manner; i. e., by partial differentiation.

Two cases need to be considered for the practical application of the Martian gravitational formulas. If one considers a fixed point above or at the surface of Mars which does not rotate with the planet, the application of the formulas is straightforward. If, however, one considers a point that rotates with the planet so that it is always directly above the same point on the Martian surface, the formulas must be corrected to account for the centrifugal acceleration of rotation.

The centrifugal correction to the radial component of gravitational acceleration can be expressed as

$$F_c = \omega^2 r \cos^2 \theta$$

in which ω is the Martian angular velocity, 0.70882×10^{-4} radians/sec.

3.8 ALBEDO

The albedo of a planet is defined as the ratio of radiant energy reflected in all directions to the incident radiant energy. Its value is required for planetary and near planetary satellite heat balance equations. For the planets themselves, the albedo is required to determine the solar radiant energy input; for near planetary satellites, the reflected albedo radiation contributes significantly to the total radiant energy input.

Earth-based albedo measurements are limited to those wavelengths which pass through the atmospheric windows. Radiation in these wavelengths contains a large percentage of the sun's total radiant energy; therefore, it appears reasonable to approximate the Martian albedo by its visual albedo.

Table 3-7 presents thermal and albedo radiation upon a spherical satellite as a function of altitude.

Table 3-8 presents planetary albedo as a function of wavelength.

Table 3-5. RADIATION VERSUS ALTITUDE

Mars Thermal and Albedo Radiation Upon a Spherical Satellite		
Albedo = 0.15; Solar Radiation = 600 watts/m ² ;		
Thermal Radiation Flux = 128 watts/m ²		
Altitude (km)	Thermal, watts/m ²	Albedo, watts/m ²
200	168	122
400	140	99
600	120	84
1000	93	63
4000	29	24
8000	11	7
20000	3	2

Table 3-6. PLANETARY ALBEDO

Wavelength, Microns	Albedo	Wavelength, Microns	Albedo
0.40	0.035	0.80	0.295*
0.45	0.065	0.90	0.30*
0.50	0.085	1.00	0.295*
0.55	0.12	1.10	0.28*
0.60	0.21	1.20	0.27*
0.65	0.25	1.3	0.255*
0.70	0.27	1.4	0.24*
0.75	0.29		

*Estimated

BIBLIOGRAPHY

- 1 Roberts, W. T., and G. S. West, The Atmosphere of Mars: A Derivation of Engineering and Design Parameters, NASA TM X-53484, MSFC, Huntsville, Alabama, June 29, 1966.
- 2 Vachon, D. N., The Density Structure of the Upper Atmosphere of Mars, Report R62SD58, Space Sciences Laboratory, General Electric Company, Valley Forge, Pennsylvania, May 1962.
- 3 Goody, R. M., The Atmosphere of Mars, Journal of the British Interplanetary Society, Vol. 16, No. 2, April - June 1957.
- 4 Coulson, K. L., and M. Lotman, Molecular Optical Thickness of the Atmosphere of Mars and Venus, Report R62SD71, Space Sciences Laboratory, General Electric Company, Valley Forge, Pennsylvania, July 1962.
- 5 Schilling, G. F., Engineering Model Atmosphere of Mars, Contract AF 49/638/-700, Rand Corporation, Santa Monica, California, September 1962.
- 6 Gross, S. H., W. E. McGovern, and S. I. Rasool, Mars: Upper Atmosphere, Science, Vol. 151, March 1966.
- 7 Donahue, T. M., Upper Atmosphere and Ionosphere of Mars, Science, Vol. 152, May 1966.
- 8 Anderson, A. D., A Model for the Lower Atmosphere of Mars Based on Mariner IV Occultation Data, Report 6-75-65-62, Lockheed Palo Alto Research Laboratory, Lockheed Aircraft Company, Palo Alto, California, December 1965
- 9 Belton, M. J. S. and D. M. Hunten, The Abundance and Temperature of CO₂ in the Martian Atmosphere, Astrophysics Journal, Vol. 145, page 454, 1966.
- 10 Spencer, D. F., Our Present Knowledge of the Martian Atmosphere, JPL Report prepared for NASA under Contract No. NAS7-100.

BIBLIOGRAPHY (Continued)

- 11 Prabhakara, C., and J. S. Hogan, Ozone and Carbon Dioxide Heating in the Martian Atmosphere, Journal of the Atmospheric Sciences, Vol. 22, No. 2, March 1965.
- 12 Kuiper, Gerard P., The Atmospheres of Earth and Planets, Revised Edition, University of Chicago Press, 1957.
- 13 Smith, R., (Editor), Space Environment Criteria Guidelines for Use in Space Vehicle Development (1967 Revision), NASA TM X-53521, MSFC, Huntsville, Alabama, February 1, 1967.
- 14 Johnson, F. S., The Atmosphere of Mars, Science, Vol. 150, page 1445, 1965.
- 15 Chamberlain, J. W. and M. B. McElroy, Martian Atmosphere, The Mariner Occultation Experiment, Science, Vol. 152, page 21, No. 2718, April 1, 1966.
- 16 Smith, O. E. and D. K. Weidner, A Reference Atmosphere for Patrick AFB, Florida, Annual (1963 Revision), NASA TM X-53139, MSFC, Huntsville, Alabama, September 23, 1964.
- 17 Jacchia, L. G., Static Diffusion Models of the Upper Atmosphere with Empirical Temperature Profiles, Research in Space Science Special Report No. 170, Smithsonian Institution, Astrophysical Observatory, December 30, 1964.
- 18 Daniels, G. E., J. R. Scoggins, and O. E. Smith, Terrestrial Environment (Climatic) Criteria Guidelines for Use in Space Vehicle Development, 1966 Revision, NASA TM X-53328, MSFC, Huntsville, Alabama, May 1, 1967.
- 19 Office Memorandum, Design Criteria - Atmospheric Models, R-AERO-YS-9-67, MSFC, Huntsville, Alabama, March 13, 1967.
- 20 Weidner, Don K., A Preliminary Summary of the MSFC Planetary Atmosphere Computer Program, NASA R-AERO-In-5-67, (Internal Note), MSFC, Huntsville, Alabama, June 30, 1967.

BIBLIOGRAPHY (Continued)

- 21 Ohring, G., and J. Mariano, Seasonal and Latitudinal Variations of the Average Surface Temperature and Vertical Temperature Profile on Mars, Final Report, Contract No. NASW-1227, GCA Corporation, Bedford, Massachusetts, March 1967.
- 22 DeVaucoulers, G., Physics of the Planet Mars, Faber and Faber Limited, 24 Russell Square, London.

APPROVAL

TM X-53616

NATURAL ENVIRONMENT DESIGN CRITERIA GUIDELINES
FOR MSFC VOYAGER SPACECRAFT FOR MARS 1973 MISSION

Edited by Don K. Weidner and C. L. Hasseltine

The information in this report has been reviewed for security classification. Review of any information concerning Department of Defense or Atomic Energy Commission programs has been made by the MSFC Security Classification Officer. This report, in its entirety, has been determined to be unclassified.

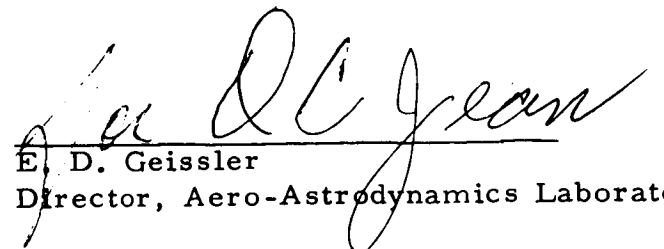
This document has also been reviewed and approved for technical accuracy.



Robert E. Smith
Chief, Space Environment Branch



W. W. Vaughan
Chief, Aerospace Environment Division



E. D. Geissler
Director, Aero-Astrodynamic Laboratory